



UNIVERSITI
TEKNOLOGI
PETRONAS

FINAL YEAR PROJECT

**DEVELOPMENT OF A NEW PACKING ELEMENT IN PACKED BED
ABSORBER**

PREPARED BY:

CHONG EE PIN

13777

SUPERVISED BY:

PROFFESOR DUVVURI SUBBARAO

Preliminary report submitted in partial fulfilment of the requirements for Bachelor of
Engineering (Hons)

(Chemical Engineering)

May 2014

Universiti Teknologi PETRONAS

Bandar Seri Iskandar

31750 Tronoh

Perak Darul Ridzuan

CERTIFICATION OF APPROVAL

Development of a New Packing Element in Packed Bed Absorber

by

Chong Ee Pin

A project dissertation submitted to the

Chemical Engineering Department

Universiti Teknologi PETRONAS

in partial fulfilment of the requirement for the

BACHELOR OF ENGINEERING (Hons)

(CHEMICAL ENGINEERING)

Approved by:

.....

(Prof Dr Duvvuri Subbarao)

UNIVERSITI TEKNOLOGI PETRONAS

TRONOH, PERAK

May 2014

CERTIFICATION OF ORIGINALITY

I hereby certify that I am responsible for the work submitted in this project, that the original work is my own except as specified in the references and acknowledgements, and that the original work contained herein have not been undertaken or done by unspecified sources or persons to the extent of my knowledge and information.

.....
(CHONG EE PIN)

ABSTRACT

The aim of this experiment is to develop a new type of packing element that can overcome the drawbacks of the current packing elements in the market for packed bed absorbers. The concept for the new packing element is making a rigid structure that holds the flexible structure together. This flexible structure should be fine and thin in order to give maximum mass transfer area while the rigid structure is to provide the strength to the packing element.

The new type of packed bed is developed by using wire gauze of 0.1 cm shaped into a spring or helix shape and attached to a rod. The concept of this idea is that the spring will move up and down as the water and dry air are mixed together in the column. These movements is hoped to increase the area of transfer for mass transfer to take place.

After the development of the new packing element, experiments are carried in a self-developed column with air and water as the medium. Water is fed from the top of the column while air is fed from the bottom. Both of them will counter-currently in contact. The pressure drop and mass transfer coefficient is then determined.

The pressure drop for Helix Prime is high when compared with the other packing elements. 2 units of Helix Primes give almost two times the pressure drop of 1 unit of Helix Prime. Although the pressure drop is high for the Helix Prime, it is still in the acceptable region of 250 Pascal. From mass transfer rate and coefficient, 1 unit of Helix Prime is inferior to the other packing elements I the industry in terms of effective interfacial for mass transfer, volumetric mass transfer coefficient and liquid phase mass transfer coefficient. However, the results were different when 2 units of Helix Prime were bind together in parallel. The mass transfer rate and coefficients are comparable with those of the Bialecki Ring Metal 25mm, VSP Ring Metal 32mm, Pall Ring metal 25mm and Hiflow Metal 27mm. 2 units of Helix Prime is a performing better than 1 unit of Helix Prime. Overall, Helix Prime is comparable with the other packing elements in the industry.

ACKNOWLEDGEMENT

First and foremost, I would like to thank the Lord for his protection throughout the conduction of my Final Year Project. It was with His protection that I was able to finish the project successfully.

Besides, I would like to take this opportunity to show my deepest appreciation to Professor Duvvuri Subbarao for his constant advice, support, assistance and guidance to me in Final Year Project for Universiti Teknologi PETRONAS. Without him, I would not have completed the project with ease. He assigned me with a very interesting topic that applied my chemical engineering knowledge which I have learnt in the past 4 years of my bachelor degree. I also benefitted a lot in terms of knowledge and also the ways of life through the constant discussions with him.

I am grateful to the lab technicians who helped me with the lab application and lab working procedures in order for me to conduct my final year project in a conducting environment and manner.

Lastly, a special thanks to my beloved parents who supported me and encouraged me during this Final Year Project. They are the pillar of strength for me to complete this project.

Thank you.

TABLE OF CONTENTS

CERTIFICATION OF APPROVAL	i
CERTIFICATION OF ORIGINALITY	ii
ABSTRACT.....	iii
ACKNOWLEDGEMENT	iv
LIST OF FIGURES	vii
LIST OF TABLES	ix
NOMENCLATURE	x
INTRODUCTION	1
1.1 BACKGROUND OF STUDY	1
1.2 PROBLEM STATEMENT	3
1.3 OBJECTIVES	4
1.4 SCOPE OF STUDY	4
LITERATURE REVIEW	5
2.1 MASS TRANSFER	5
2.2 PRESSURE DROP	9
2.3 WETTED WICK	11
METHODOLOGY	12
3.1 PROCESS FLOW CHART	12
3.2 GANTT CHART AND KEY MILESTONE	13
3.3 EXPERIMENTAL METHODOLOGY	15
3.3.1 Designing the New Type of Packing Elements.....	15
3.3.1.1 Prototype- Helix Prime	15
3.3.2 Experimental Setup.....	17
3.2.2.1 Orifice Flow Meter Design	20
3.3.3 Experimental Procedure	23
RESULTS AND DISCUSSION	24
4.1 PACKING CHARACTERISTICS	24
4.2 PRESSURE DROP	25
4.3 MASS TRANSFER EFFICIENCY	30

CONCLUSION AND RECOMMENDATION	37
5.1 CONCLUSION	37
5.2 SUGGESTED FUTURE WORK FOR EXPANSION AND CONTINUATION ...	38
REFERENCE.....	39
APPENDICES	40

LIST OF FIGURES

Figure 1: Packed bed absorber.....	1
Figure 2: Raschigs rings.....	2
Figure 3: Structured packing.....	3
Figure 4: Development of random packing element.....	4
Figure 5: The first prototype – Helix Prime.....	15
Figure 6: Connection of wire onto the rod of Helix Prime.....	16
Figure 7: Basic flow diagram of the experimental setup.....	17
Figure 8: Experimental setup.....	18
Figure 9: Gas inlet with digital thermometers.....	19
Figure 10: Gas outlet with digital thermometers.....	19
Figure 11: Orifice flow metre pressure difference manometer.....	19
Figure 12: Column pressure drop manometer.....	19
Figure 13: Basic flow diagram of orifice flow meter.....	20
Figure 14: Graph of Pressure Drop versus Superficial Gas Velocity for 1 Unit Helix Prime at operational condition.....	25
Figure 15: Graph of Pressure Drop versus Superficial Gas Velocity for 2Units of Helix Prime at operational condition.....	26
Figure 16: Graph of Friction Factor Reynolds number versus Reynolds number of Helix Prime.....	28

Figure 17: Graph of Pressure Drop of Packing versus Superficial Gas Velocity for different packing.....	29
Figure 18: Experimental data for volumetric mass transfer coefficient, $\beta_L a_e$, as a function of specific liquid load, μ_L	31
Figure 19: Graph of effective interfacial area for mass transfer per unit volume versus specific liquid load for different types of packing elements.....	32.
Figure 20: Graph of volumetric mass transfer coefficient versus specific liquid load for different types of packing elements.....	33
Figure 21: Graph of liquid phase mass transfer coefficient versus specific liquid load for different types of packing elements.....	34
Figure 22: Graph of experimental results of gas phase mass transfer coefficient versus gas flow rate at fixed water flow rate of 0.022 m/s.....	35
Figure 23: Graph of experimental results of Sherwood number versus Reynolds number at fixed water flow rate of 0.022 m/s.....	36

LIST OF TABLES

Table 1: Overview of technical data of packing used for calculating volumetric mass transfer coefficient, $\beta_{L,a}$	8
Table 2: Gantt chart and key milestone for FYP I.....	13
Table 3: Gantt chart and key milestone for FYP II.....	14
Table 4: Characteristic of Helix Prime.....	16
Table 5: Basis of design for the orifice flow meter.....	22
Table 6: Characteristics of different packing elements.....	24

NOMENCLATURE

- η_A = Mass transfer rate [mol/s]
 k_C = Mass transfer coefficient [m/s]
 A = Effective mass transfer area [m²]
 ΔC_A = Driving force concentration difference [mol/m³]
 β_L = Liquid-phase mass transfer coefficient [m/s]
 a_e = Effective interfacial area for mass transfer per unit volume [m²/m³]
 Q_{volume} = Volumetric flow rate [m/s]
 V = Volume occupied by packing [m³]
 a = Geometric surface area of packing per unit volume [m²/m³]
 h_L = Specific liquid hold-up [m²/m³]
 d_T = Mean droplet diameter [m]
 u_L = Specific liquid load [m/s]
 d_h = Hydraulic diameter [m]
 l = Mean contact path [m]
 ϕ_p = Form factor [-]
 τ = Contact time [s]
 $\Delta\rho, \rho_L - \rho_V$ = Differential density [kg/m³]
 σ_L = Surface tension of liquid [N/m]
 ν_L = Kinematic viscosity [m²/s]
 Re_L = Reynolds Number [-]
 g = Gravitational acceleration, 9.81 m²/s
 D_L = Diffusion coefficient of liquid [m²/s]
 Δp = Pressure drop across the packed bed (kg/m.s)
 L = Length of the packed bed (m)
 D_p = Equivalent spherical diameter of the packing (m)
 ρ = Density of fluid (kg/m³)
 μ = Dynamic viscosity of the fluid (kg/m.s)
 V_S = Superficial velocity of fluid (m/s)
 ε = Void fraction

CHAPTER 1

INTRODUCTION

1.1 BACKGROUND OF STUDY

Packed bed columns are widely used in many industries to perform separation processes such as stripping, distillation and also absorption. Besides, they are also used in chemical reactors to catalyze gas reaction with solid catalyst. As shown in **Figure 1**, a packed bed is a hollow vessel filled with a certain type of packing material that improves the contact time between two phases or fluids in a chemical process. This is achieved by providing a wide surface area for contact between the fluids for rapid heat and mass transfer.

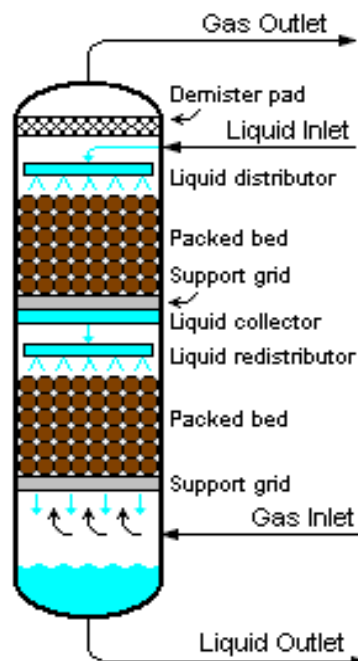


Figure 1: Packed bed absorber (courtesy of Hatford)

For a typical packed bed absorber, the liquid solvent is distributed evenly across the packing by a liquid distributor at the top of the packed bed column. This liquid will flow down and counter-currently be in contact with the gas that is fed from the bottom of the column. The liquid-soluble impurities from the gas are transferred to the liquid solvent flowing down the column while the lean gas leaves the column at the top.

Packed bed can be categorized into two types:

- Structured packed bed
- Random packed bed



Figure 2: Raschig rings



Figure 3: Structured packing

For random packed beds, the packed bed is randomly filled with small rigid objects like the Raschig rings (**Figure 2**) while structured packed bed (**Figure 3**) has a structured organization of the packing elements such as thin corrugated metal plates. Both of these give a large surface area for mass transfer between the fluids. Random dumped packing displays process properties approximately the same as the structured packing and is able to meet the advantages of mass transfer tray (Schultes, 2003). This statement creates a platform for the development of modern random dumped packing based on the studies of mass transfer.

1.2 PROBLEM STATEMENT

The development of packing elements for packed bed absorbers had great impacts on the chemical industry especially in the field of separation processes. Since the introduction of the first generation packing such as Raschig Rings and Berl-Saddle in 1895, the development of new packing had been rapid and currently the industries packed columns are packed with the fourth generation Raschig Super Rings. The figure below depicts the development of the random packing element since its first introduction to the industry in 1895.

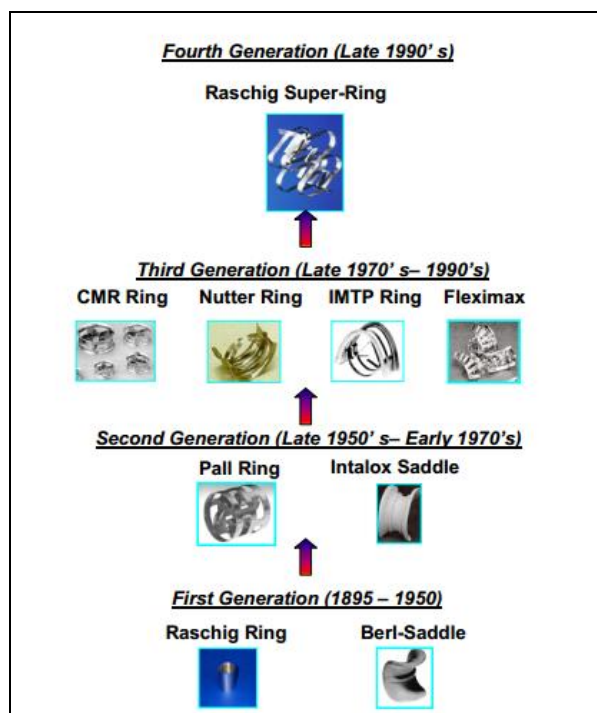


Figure 4: Development of random packing element. (Schultes, 2003)

The first generation packing involves the usage of rigid structure as the packing element. As the understanding on packing elements and mass transfer improved, the structure of the packing evolves from a rigid structure to a more flexible structure such as the Raschig Super Rings. The new generation packing gives a larger mass transfer area compared to the first generation packing and hence improves the efficiency of the process. Even though the new packing provides higher mass transfer area, the flexible structure of the element allows it to get crushed or deformed at the bottom of the column due to the column weight if the packing is too

high. Therefore, the challenge for us is to develop the next generation of packing element that can address the drawbacks of the new generation of packing element. The idea for the next generation can start with the combination of rigid and flexible structure for the packing element. The rigid structure is expected to provide the support for the flexible structure, which provides a larger surface area for mass transfer. On top of that, the flow of gas can be manipulated to flow cross-counter currently to increase the time of contact with the liquid solvent flowing down the column. This next generation packing element is also expected to be able to compete against industrially recognized random dumped and structured packing available in the market.

1.3 OBJECTIVES

The purpose for conducting this research is listed as below:

- i. To develop a new design or type of packing element for packed bed column
- ii. To study the characteristics and performance of the newly developed packing element.
- iii. To compare the newly developed packing element with the existing packing elements in the market.
- iv. To ease the cleaning of the packed bed column.

1.4 SCOPE OF STUDY

The scope of study can be simplified as follow:

- i. The combination of rigid and flexible structure for a new random dumped packing element.
- ii. The mass transfer between the liquid and gas of the new packing element.
- iii. The pressure drop along the new packed bed column.
- iv. The development of a new packing element..
- v. The performance characteristics of the new packing element.

CHAPTER 2

LITERATURE REVIEW

2.1 MASS TRANSFER

Mass transfer can be defined as the net movement of mass from one point to another. The driving force for mass transfer is the difference in chemical potential between areas of high chemical potential and those of lower chemical potential. It is the mechanism for packed bed absorbers.

Based on the formula for mass transfer rate:

$$\eta_A = k_c A \Delta C_A \quad [mol \ s^{-1}] \quad (1)$$

In order to achieve highest mass transfer, all the 3 parameters on the right-hand side of the equation; mass transfer coefficient, k_c , effective mass transfer area, A , and concentration difference, ΔC_A , must be maximized. Since the concentration difference is solely dependent on the process, only the mass transfer coefficient and effective mass transfer area can be affected by design of the packing element in the packed column.

Model for the prediction of liquid phase mass transfer for random packed columns for gas-liquid systems was developed by Jerzy Mackowiak in 2011. The new equation suggested by Mackowiak for the volumetric mass transfer coefficient is $\beta_{L,ae}$. This equation was derived on the assumption that the liquid flows down the packed bed mainly in the form of droplets and the effective interfacial area per unit volume, a_e depends solely on the hold up in the packed bed (Mackowiak, 2011).

By combining the liquid phase mass transfer coefficient, β_L and the effective interfacial area per unit volume, a_e , into equation (1), the volumetric mass transfer coefficient can be formed.

$$\eta_A = k_c A \Delta C_A = \beta_L a_e V \Delta C_A \quad [mol \ s^{-1}] \quad (2)$$

The effective mass transfer area, A in equation (1) is the same as the product of the effective interfacial area for mass transfer per unit volume, a_e , and the volume occupied by the packing, V . According to Mackowiak (2011), the effective mass transfer area per unit volume, a_e , is identical to the droplet surface, while the total liquid hold up, h_L , corresponds to the liquid hold-up of the droplets. The interfacial area per unit volume can be determined by using the following equation:

$$a_e = 6 \frac{h_L}{d_T} \quad [m^2 / m^3] \quad (3)$$

The specific liquid hold-up is dependent on the flow regime across the packed bed. The flow regime can be determined through Reynolds number, Re_L , with the following formula:

$$Re_L = \frac{\mu_L}{av_L} \quad [-] \quad (4)$$

According to Mackowiak (2010), the specific liquid hold-up, h_L , in random packing for turbulent flow, $Re_L \geq 2$:

$$h_L = 0.57 \left(\frac{\mu_L^2 a}{g} \right)^{1/3} \quad [m^2 / m^3] \quad (5)$$

For lamina flow, $0.16 < Re_L < 2$:

$$h_L = 0.75 \left(\frac{3}{g} \right)^{1/3} a^{2/3} (\mu_L v_L)^{1/3} \quad [m^2 / m^3] \quad (6)$$

Based on equation (3), (5) and (6), the effective interfacial areas per unit volume, a_e is directly proportional to the geometric surface area of packing per unit volume, a . Therefore, a packing design with high surface area will provide a higher effective interfacial area for mass transfer.

The mean droplet diameter in accordance to the Sauter mean of the droplets can be determined using:

$$d_T = \sqrt{\frac{\sigma_L}{\Delta\rho g}} \quad [\text{m}] \quad (7)$$

According to Higbie (1935), the formula for determining liquid phase mass transfer coefficient can be described by:

$$\beta_L = \frac{2}{\sqrt{\pi}} \sqrt{\frac{D_{:L}}{\tau}} \quad [\text{m/s}] \quad (8)$$

This equation can be used if the contact time τ of the droplet to cover the distance, l , between two contact-points within the packing (Schultes, 2011).

$$\tau = \frac{l}{\bar{u}_L} \quad [\text{s}] \quad (9)$$

The absolute droplet velocity can be expressed by:

$$\bar{u}_L = \frac{u_L}{h_L} \quad [\text{m/s}] \quad (10)$$

Substituting equation (10) in equation (9),

$$\tau = \frac{l \cdot h_L}{u_L} \quad [\text{s}] \quad (11)$$

Mackowiak (2010) expressed a correlation for the contact path, l . This correlation is expressed as:

$$l = 0.155(1 - \varphi_p)^{2/3} d_h^{1/2} \quad [\text{m}] \quad (12)$$

For the hydraulic diameter, d_h , the following formula is used:

$$d_h = \frac{4\varepsilon}{a} \quad [\text{m}] \quad (13)$$

Table 1: Overview of technical data of packing used for calculating volumetric mass transfer coefficient, $\beta_{L,ae}$ (Mackowiak, 2011).

Packing	Symbol	$d \times 10^3$ (m)	ε (m ³ /m ³)	a (m ² /m ³)	$N \times 10^3$ (1/m ³)	d_s (m)	H (m)	$u_L \times 10^3$, from-to (m/s)	t_L (°C)	φ_P (-)
(a) Classic, non-perforated packing elements										
Raschig ring	◊	15	0.626	239.3	–	0.10	1.0	1.7–11	20–40	0
Ceramic	◆	50	0.782	100	6300	0.3	0.75	1–22.5	20	0
Intalox saddle ceramic	◊	38	0.757	125.7	18.9	0.3	1.4	1–11	21	0
(b) Packing elements with slightly perforated walls										
Pall ring metal	○	15	0.964	380	243.2	0.3	0.87	1–11	22.5	0.28
	○	25	0.954	223.5	53.9	0.3	1.46	1–11	21.5	0.28
	○	$s=0.4$	0.942	232.1	55.6	0.15	1.3	0.79–10	22.5	0.28
Pall ring plastic (PP)	○	25	0.946	150	19.6	0.3	1.4	1.2–8	19.5	0.28
	○	38	0.952	149.6	15.8	0.3	1.46	1–11	20	0.28
	○	50	0.95	115.4	6.4	0.3	1.36	1–12	22.5	0.28
Pall ring ceramic	□	25	0.894	238	55.18	0.3	1.4	1–10	23	0.309
	□	35	0.905	160	18	0.3	1.4	1–10	20	0.309
	■	50	0.93	111	6.85	1.0	1.65	1–18	20	0.309
Bialecki ring metal	□	50	0.92	110	6.7	0.3	1.35	1–15	22	0.309
	□	50	0.78	120	6.4	0.22	1	1–12	20	0.430
	■	12	0.934	403	443	0.3	0.9	1–11	17.5	0.158
Bialecki ring metal	⊠	25	0.94	238	55	0.15	1.5	0.79–28	20	0.208
	⊠	25	0.939	227	52.6	0.3	1.4	1–7	22	0.208
	⊠	35	0.95	155	19	0.3	0.74	2–30	17.5	0.158
	⊠	50	0.97	111.7	6.7	0.3	1.45	1–11	20	0.158
	⊠	53.5	0.968	101.5	6	0.3	1.2–1.4	0.8–28	16.5	0.208

The volumetric mass transfer coefficient, $\beta_{L,ae}$, can be obtained by substituting equation (5) to (7) into equation (3) and equation (5), (6), (11) and (12) into equation (8).

For turbulent flow, $Re \geq 2$:

$$\beta_{L,ae} = \frac{15.1}{(1-\varphi_p)^{1/3} d_h^{1/4}} \left(\frac{D_L \Delta \rho g}{\sigma_L} \right)^{1/2} \left(\frac{a}{g} \right)^{1/6} u_L^{5/6} \quad [1/s] \quad (14)$$

For laminar flow, $0.16 < Re < 2$:

$$\beta_{L,ae} = \frac{17.3 a^{1/3}}{(1-\varphi_p)^{1/3} d_h^{1/4}} \left(\frac{D_L \Delta \rho g}{\sigma_L} \right)^{1/2} \left(\frac{3v_L}{g} \right)^{1/6} u_L^{2/3} \quad [1/s] \quad (15)$$

Based on equation (14) and (15), the volumetric mass transfer coefficient is proportional to the geometric surface area of the packing per unit volume, a . Thus, the design of the packing will affect the mass volumetric mass transfer coefficient and also the mass transfer rate.

2.2 PRESSURE DROP

Pressure drop along the packed bed is one of the important parameters that determine the performance and feasibility of the packing element. Low pressure drop during process or operation is favoured because it provides stability in the system and also reduces the energy consumption of the compressor to move gas long the packed column. A typical equation that is used to estimate the pressure drop along the packed bed column is the Ergun's equation (1952).

$$f_p = \frac{150}{Gr_p} + 1.75 \quad [-] \quad (16)$$

where

$$f_p = \frac{\Delta p D_p}{L \rho V_s^2} \left(\frac{\varepsilon^3}{1 - \varepsilon} \right) \quad [-] \quad (17)$$

$$Gr_p = \frac{D_p V_s \rho}{(1 - \varepsilon) \mu} \quad [-] \quad (18)$$

Substitute (3) and (4) into (2) and rearranging, we obtain the pressure drop across the packed bed:

$$\Delta p = \frac{150 \mu (1 - \varepsilon)^2 V_s L}{D_p^2 \varepsilon^3} + \frac{1.75 \rho V_s^2 L (1 - \varepsilon)}{D_p \varepsilon^3} \quad [\text{kg/m}] \quad (19)$$

Where

Δp is the pressure drop across the packed bed

L is the length of the packed bed

D_p is the equivalent spherical diameter of the packing

ρ is the density of the fluid

μ is the dynamic viscosity of the fluid

V_s is the superficial velocity

ε is the void fraction of the bed

Based on equation (19), the pressure drop across a packed bed is inversely proportional to the void fraction of the bed, ε , and the equivalent spherical diameter of the packing element, D_p . For a packing with high void fraction and large equivalent spherical diameter of the packing element, the pressure drop across the packed bed will be very small and can be negligible.

Besides, the pressure drop across a packed bed is directly proportional to the superficial velocity of fluid, density of fluid, and the length of packed bed in the column. In normal system, the density of the fluids are constant throughout the system, the variables will then be the packed bed column length and superficial velocity of fluid. Therefore, a column with long packed bed will have a higher pressure drop compared to column with shorter packed bed. Operation at high liquid and gas loading will cause high pressure drop across the packed bed.

If the system differs from that of Ergun's condition, the equation can be expressed as:

$$\frac{\Delta p}{L} \frac{D_p}{\rho V_s^2} \left[\frac{\varepsilon^3}{(1-\varepsilon)^2} \right] \left(\frac{D_p V_s \rho}{\mu} \right) = \left[\left(\frac{D_p V_s \rho}{(1-\varepsilon)\mu} \right) \right] k_2 + k_1 \quad [-] \quad (20)$$

The constant k_2 describes the turbulence flow relation with the pressure loss across the packed bed, while k_1 describes the laminar flow relation of the pressure loss across the packed bed. These two values can be calculated and compared for different packing elements. The common value for k_2 ranges between 1.5 and 1.8, while the common value for k_1 ranges between 150 and 180.

2.3 WETTED WICK

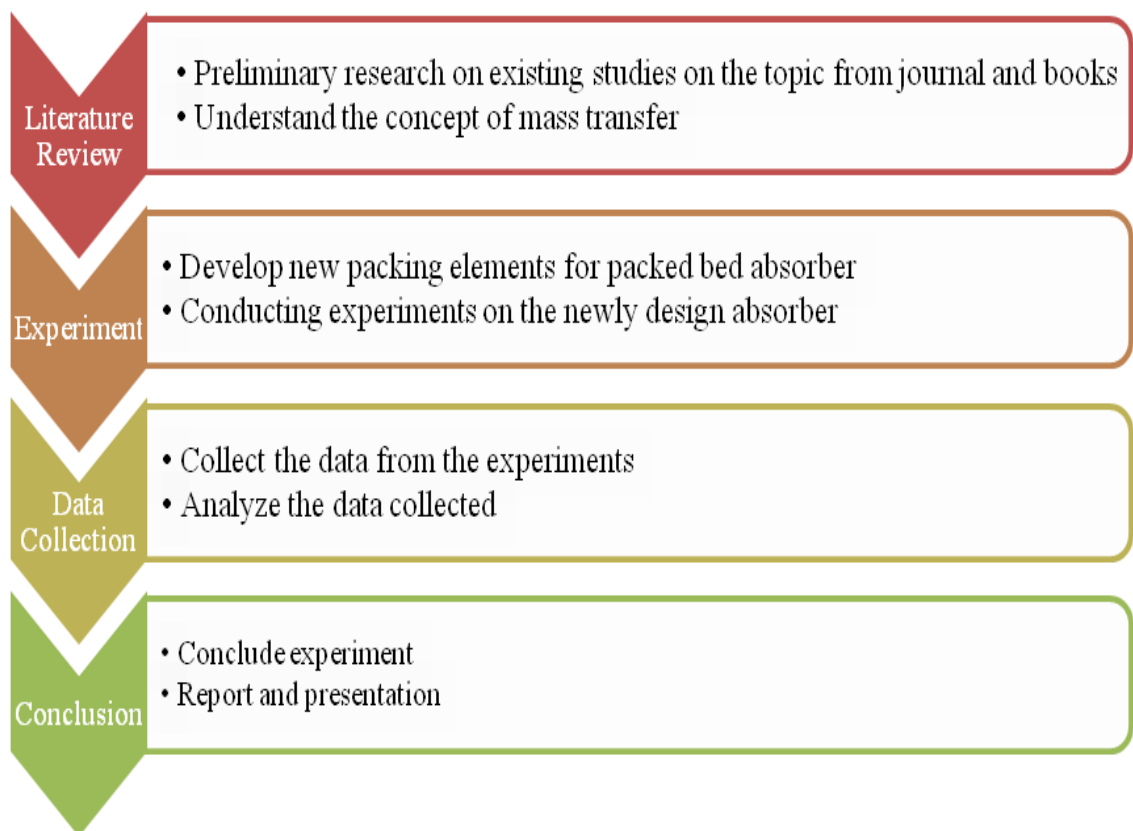
The construction of a packing element using wick is a best example for mass transfer through flexible structures. It has a high wettability and based on the materials that it is constructed, wicks can provide a high mass transfer area for mass transfer. Lee and Hwang (1989) conducted a series of experiments on a newly designed column called the wetted wick column. In this column, the inner surface of the wetted wick column is covered with a layer of capillary-porous materials supported by wire clothes and is wetted with a liquid solvent. They used cotton fibre glass and wire mesh as materials for the wick in the column. The wicks are used to provide large surface area for mass transfer and thus increase the efficiency for mass transfer. According to Lee and Hwang (1989), the wetted wick column has the following characteristic:

- Provides 100% wetted surface even at low liquid flow rate
- Fairly low pressure drop
- Uniform distribution of liquid across the packing
- Neglect wall flow of fluid
- Does not create back-mixing which can cause bad mass transfer
- Can be operated in the absence of gravity

CHAPTER 3

METHODOLOGY

3.1 PROCESS FLOW CHART



3.2 GANTT CHART AND KEY MILESTONE

Table 2: Gantt chart and key milestone for FYP I

Task	Week													
	1	2	3	4	5	6	7	8	9	10	11	12	13	14
Topic selection	■	■												
First meeting with supervisor		■												
Preliminary Research Work		■	■	■	■									
Submission of Extended Proposal						●								
Proposal defence							●							
Developing new packing element							■	■	■	■	■	■	■	■
Planning of experimental procedure										■	■	■	■	■
Submission on interim draft report													●	
Submission of interim report														●

Milestone ● Process ■

Table 3: Gantt chart and key milestone for FYP II

Task	Week													
	1	2	3	4	5	6	7	8	9	10	11	12	13	14
Conducting Experiments	■	■	■	■	■	■	■	■						
Calculations for Experiments		■	■	■	■	■	■	■						
Submission of Progress Report								●						
Continuation of work									■	■	■	■		
Pre-Sedex										●				
Submission of Draft Final Report											●			
Submission of Dissertation (soft bound)												●		
Submission of Technical Paper												●		
Viva Voce													●	
Submission of Project Dissertation (hard bound)														●

Milestone ● Process ■

3.3 EXPERIMENTAL METHODOLOGY

3.3.1 Designing the New Type of Packing Elements

The new generation of packing element should comprise of the rigid structure from the previous generations and the flexible structure of the new generation. The work of Lee and Hwang (1989) gave us the basic for the new design. Rigid structure is expected to provide the strength to hold the fine flexible strands together, whereas, the strands provide the surface area for mass transfer. Providing counter current flow between the fluids can give a longer time of contact for more mass transfer.

3.3.1.1 Prototype- Helix Prime

Based on the criteria for the new generation of packing element, Helix Prime was constructed by using a commonly found object in our daily life – steel wire and plastic rod. Steel wire can be easily bought in normal hardware shops and it is cheap. The steel wire is first twisted into the shape of a spring with the aid of a wooden stick of diameter 2.3 cm. The wire is turn about 60 loops on the wooden stick before it is cut. Then the wire is connected to the plastic rod by heating the wire and piercing it through the rod. The length of the rod is measure to be 34 cm.

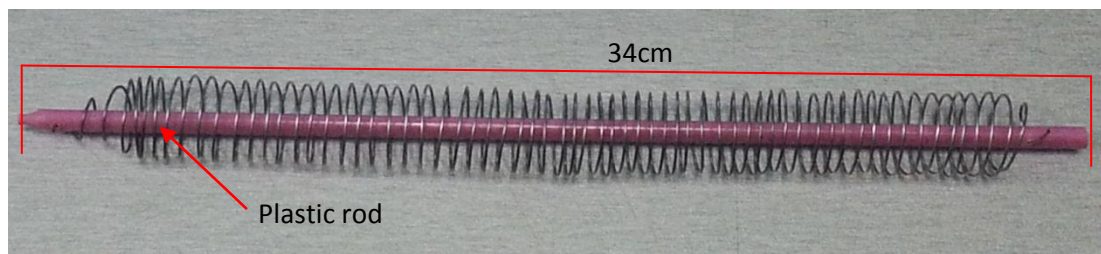


Figure 5: The first prototype – Helix Prime



Figure 6: Connection of wire onto the rod of Helix Prime

Table 4: Characteristic of Helix Prime

Characteristics	Number of Helix Prime	
	1	2
Total surface area (m^2)	0.04428	0.08783
Total volume (m^3)	1.5305×10^{-5}	3.061×10^{-5}
Geometric surface area per unit volume (m^2/m^3)	105.53	209.32
Void fraction, ε	0.9635	0.9270
Equivalent spherical diameter (m)	2.074×10^{-3}	2.091×10^{-3}

After constructing the packing element, the next step is to conduct a series of experiment to analyze the characteristics and performance of the newly developed packing element based on:

i. Hydrodynamic performance

In this part, the pressure drop along the packed column is evaluated based on the

- Pressure drop test using air-water counter current flow (wet and dry packing)
- Ergun's equation

ii. Mass transfer efficiency

In this part, the mass transfer rate, moisture content, volumetric mass transfer coefficient and wetting efficiency are evaluated based on equations and correlations obtained from the literature.

3.3.2 Experimental Setup

Both hydrodynamic and mass transfer coefficient experiment will be conducted using an air-water counter current flow experimental setup. The basic flow diagram of the experimental setup is shown in Figure 1. Water and air are used because they are readily available in the laboratory and easy to dispose.

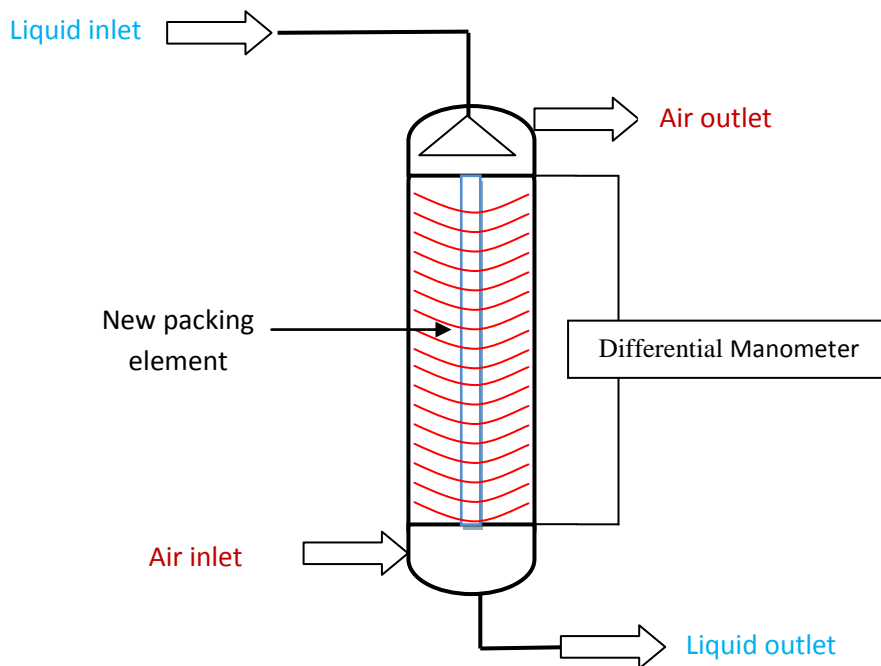


Figure 7: Basic flow diagram of the experimental setup

The column is made from PVC which is easily found in hardware shops and holes are drilled at specific places to fit the manometer. The manometer is then filled with water as the medium to detect the change in pressure.

The new packing element is placed in the middle of the column as shown in **Figure 8**. Water is then fed from the top of the column and let to flow out from the bottom while the air is fed from the bottom and exit at the top of the column.

The concept of air humidifier is used for the mass transfer experiment. By contacting air with water, some of the water will evaporate and transfer into the air causing the air humidity to increase. The humidity of the inlet and outlet air is analyzed by using the dry-bulb and wet-bulb temperature for both the inlet and outlet flow. With these temperatures, the amount of water in the air can be determined with a psychrometric chart. By calculating the humidity difference between the inlet and outlet gas, we can calculate the amount of water transferred into the air. Multiplying the amount of water evaporated with the mass flow rate, we can determine the rate of mass transfer.

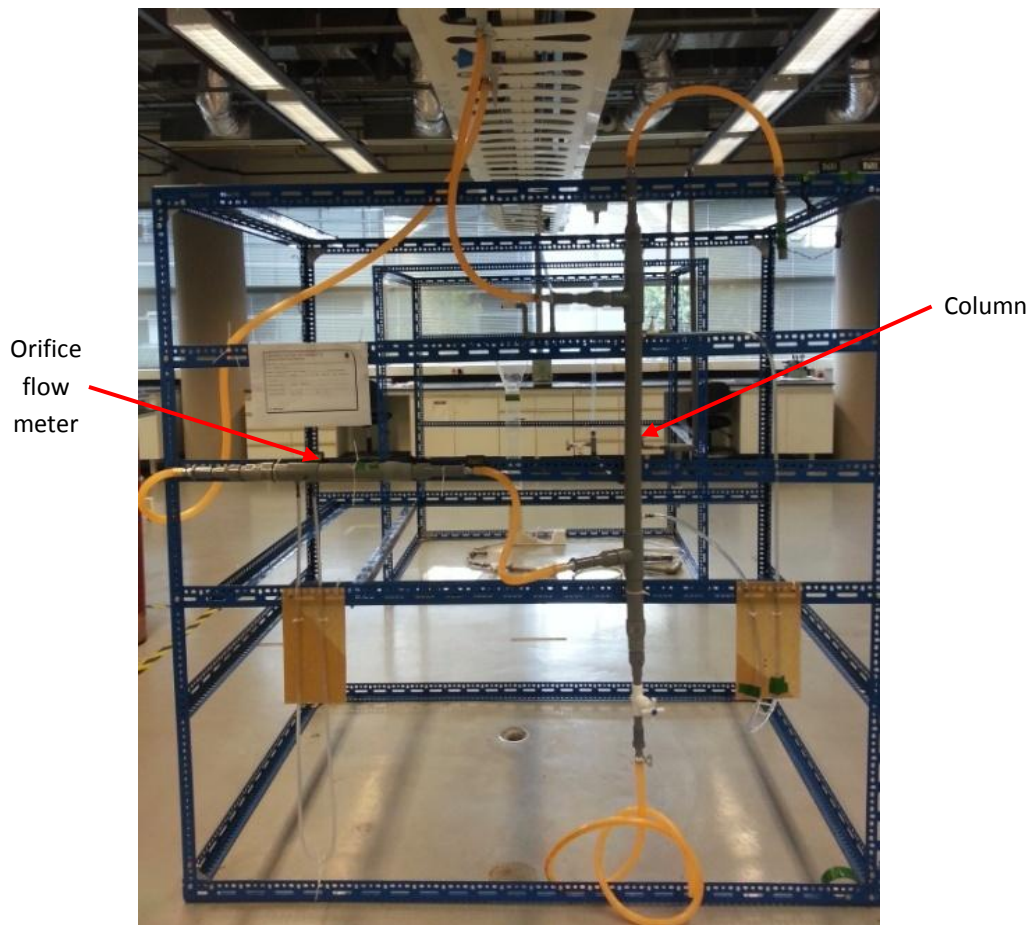


Figure 8: Experimental setup

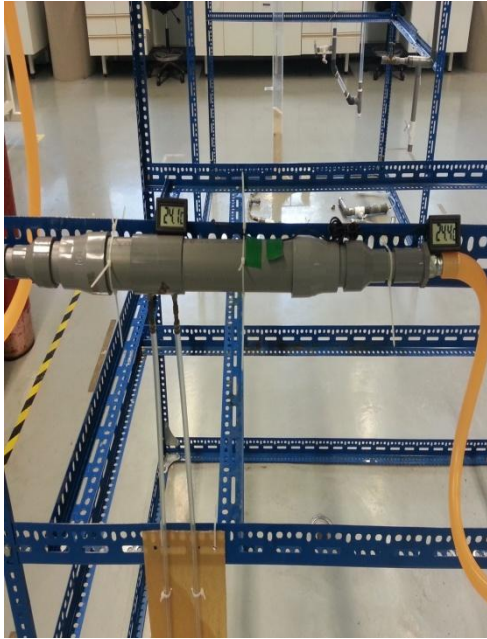


Figure 9: Gas inlet with digital thermometers



Figure 10: Gas outlet with digital thermometers



Figure 11: Orifice flow metre pressure difference manometer

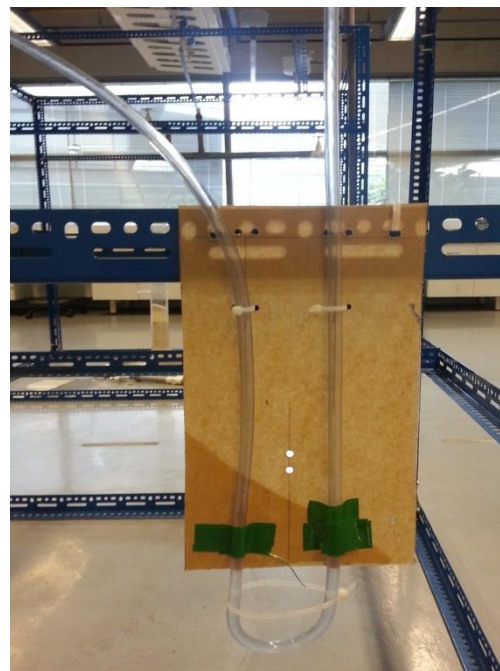


Figure 12: Column pressure drop manometer

3.2.2.1 Orifice Flow Meter Design

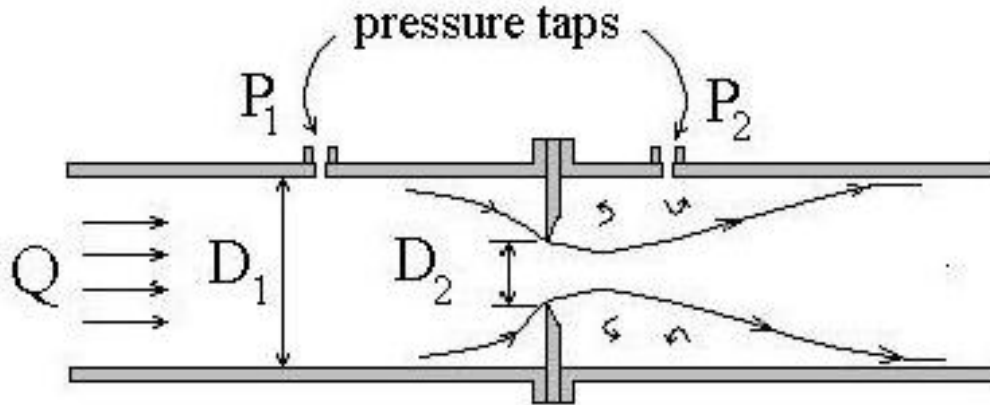


Figure 13: Basic flow diagram of orifice flow meter

In order to conduct the experiment, the inlet air flow rate through the absorber column needs to be measured. In this experiment, the fluid speed is assumed to operate below the subsonic region, thus, the incompressible Bernoulli's equation is applicable to describe the flow.

Applying the equation to a streamline travelling down the axis of the horizontal tube gives,

$$\Delta p = p_1 - p_2 = \frac{1}{2} \rho V_2^2 - \frac{1}{2} \rho V_1^2 \quad [kg/m.s] \quad (21)$$

Location 1 is the orifice diameter upstream of the orifice, and location 2 is positioned at one-half orifice diameter downstream of the orifice. From the continuity equation, the velocities can be replaced by cross-sectional areas of the flow and the volumetric flow rate, Q;

$$\Delta p = \frac{1}{2} \rho Q^2 \frac{1}{A_2^2} \left[1 - \left(\frac{A_2}{A_1} \right)^2 \right] \quad [kg/m.s] \quad (22)$$

Solving for the volumetric flow rate Q gives;

$$Q = \sqrt{\frac{2\Delta p}{\rho}} \frac{A_2}{\sqrt{1 - \left(\frac{A_2}{A_1}\right)^2}} \quad [m^3 / s] \quad (23)$$

The above equation is only applicable to perfectly laminar and inviscid flows. For real flows, viscosity and turbulence are present and act to convert kinetic flow energy into heat. To account for this effect, a discharge coefficient, C_d is introduced into the above equation to marginally reduce the flow rate Q ;

$$Q = C_d \sqrt{\frac{2\Delta p}{\rho}} \frac{A_2}{\sqrt{1 - \left(\frac{A_2}{A_1}\right)^2}} \quad [m^3 / s] \quad (24)$$

The actual flow profile at location 2 downstream of the orifice is complex, causing the effective value of A_2 uncertain. To make the calculation easier, the following substitution is made;

$$C_f A_o = C_D \frac{A_2}{\sqrt{1 - \left(\frac{A_2}{A_1}\right)^2}} \quad [m^2] \quad (25)$$

A_o is the area of the orifice. As a result, the volumetric flow rate Q for real flows is given by the equation;

$$Q = C_f A_o \sqrt{\frac{2\Delta p}{\rho}} \quad [m^3 / s] \quad (26)$$

The mass flow rate can be calculated by multiplying the volumetric flow rate with fluid density;

$$Q_{mass} = \rho Q \quad [kg / s] \quad (27)$$

For the experiment, the gas used is air. The pressure difference for the orifice is measured based on the difference in water height using a simple manometer made

of transparent tube filled with water. The following equation is used to calculate the pressure difference;

$$\Delta p = \rho g h \quad [kg / m \cdot s^2] \quad (28)$$

For this experiment, the basis design of the orifice flow meter in order to measure the air flow rate entering the packed column is summarized in the table below:

Table 5: Basis of design for the orifice flow meter

Pipe (inlet) diameter upstream of orifice D_i , cm	3.8
Pipe area upstream of orifice A_i , m^2	0.001134
Orifice diameter D_o , cm	1.3
Orifice area A_o , m^2	0.0001327
Water density, kg/m^3	1000
Gravitational constant, m/s^2	9.81
Flow coefficient, C_f	0.61

For the calculation of volumetric flow rate, the density of air can be found in the psychometric chart based on the dry-bulb and wet-bulb temperature of the inlet air.

3.3.3 Experimental Procedure

3.2.3.1 Dry Pressure Drop Experiment

1. Close the water outlet valve.
2. Open the air inlet valve until the water height in the orifice flow meter pressure difference manometer increase by 0.2cm.
3. Measure and record the water height increment in the column pressure drop manometer.
4. Repeat step 2 and 3 with water height of 0.4cm, 0.6cm, 0.8cm, 1.0cm, 2.0cm, 3.0cm and 3.5cm in the orifice flow meter pressure difference manometer.

3.2.3.2 Mass Transfer Experiment

1. Open the water outlet valve until it is fully open.
2. Fully open the water inlet valve for 10 minutes to make sure that the packing element is fully wetted.
3. Close the water inlet partially to reduce the water flow rate.
4. Collect the amount of water flowing out of the column in 10 seconds using a measuring cylinder and record the amount.
5. Close the water outlet valve partially to prevent air from escaping through the water outlet valve.
6. Attach wet tissue papers to one of the 2 digital thermometers probes that are located at the gas flow inlet and outlet respectively.
7. Open the gas inlet valve partially until the water height in the orifice flow pressure manometer increase by 0.2 cm.
8. Let the equipment run for 5 minutes and then record the wet-bulb and dry-bulb temperature of both inlet and outlet gas flow.
9. Record the water height increment in the column pressure drop manometer.
10. Repeat step 7 to 10 with water height of 0.4cm, 0.6cm, 0.8cm, 1.0cm, 2.0cm, 3.0cm and 3.5cm .

CHAPTER 4

RESULTS AND DISCUSSION

4.1 PACKING CHARACTERISTICS

Table 6: Characteristics of different packing elements (Mackowiak, 2011)

Characteristics	1 unit Helix Prime	2 units Helix Prime	Bialecki Ring Metal 25mm	VSP Ring Metal 32mm	Pall Ring Metal 25mm	Hiflow Ring Metal 27mm
<i>Geometric surface area per unit volume (m^2/m^3)</i>	105.53	209.32	227.00	200	232.10	198.4
<i>Void fraction, ε</i>	0.9635	0.927	0.939	0.972	0.942	0.965
<i>Equivalent spherical diameter of packing, D_p (m)</i>	0.002074	0.002091	0.0375	0.075	0.0375	0.0405
<i>Form factor, φ_p</i>	0.208	0.208	0.208	0.380	0.280	0.509

Based on the results from **Table 6**, the geometric surface area per unit volume for Helix Prime is comparable with Bialecki Ring Metal 25mm, VSP Ring Metal 32mm, Pall Ring Metal 25mm and Hiflow Ring Metal 27mm if two units Helix Prime are used together in parallel. One unit of Helix Prime is inferior to all the other packing elements as the geometric surface area per unit volume of the packing is considerably low.

Besides, the void fraction for two units of Helix Prime is comparable with the other packing elements, with value of 0.927. This indicates that it has a low resistance to fluids flow inside the column and thus, suggests that the pressure drop across the column could be low during the operation. Although one unit has a higher void fraction, it lacks in the geometric surface area part when compared with the other packing elements.

4.2 PRESSURE DROP

Pressure drop across the column when using the Helix Prime was obtained through the hydrodynamic tests during the operation. The experimental values are then compared with the values calculated from equation (19) - the Ergun's equation. The Ergun's constants are assumed to be $k_1 = 150$ and $k_2 = 1.75$.

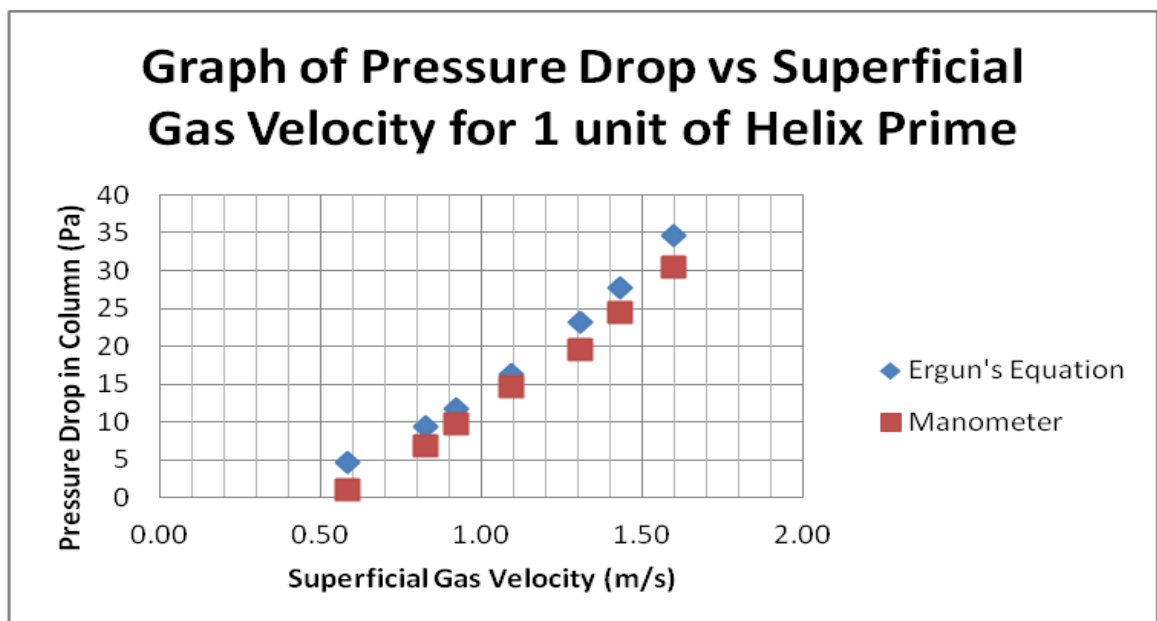


Figure 14: Graph of Pressure Drop versus Superficial Gas Velocity for **1 Unit** of Helix Prime at operational condition.

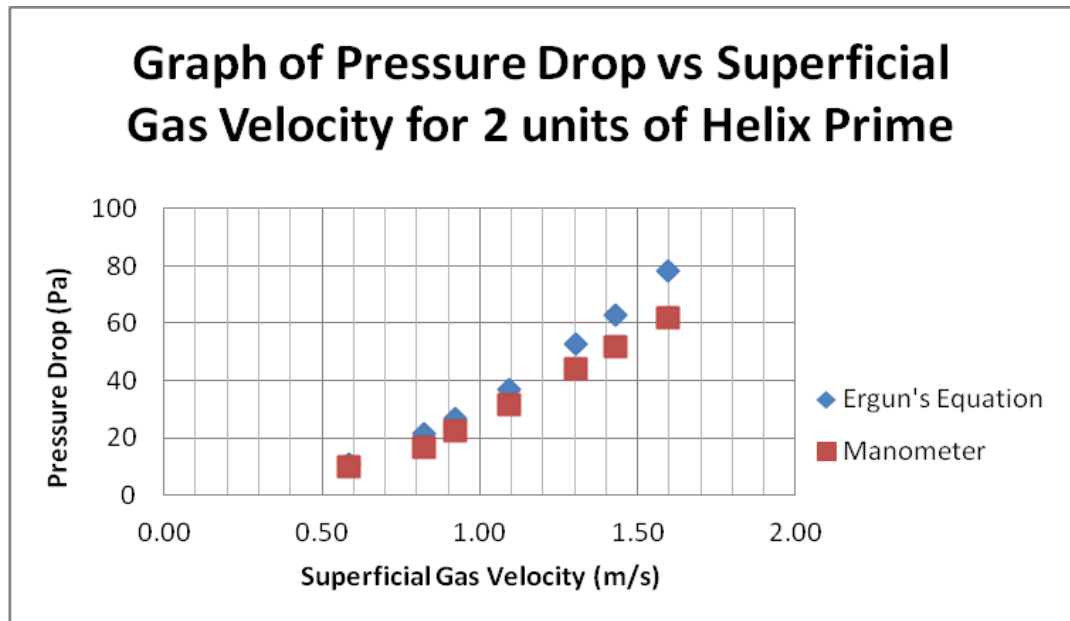


Figure 15: Graph of Pressure Drop versus Superficial Gas Velocity for **2Units** of Helix Prime at operational condition

Based on both **Figure 14** and **Figure 15** the calculated values from Ergun's equation or equation (19) are comparable with those from the experimental values. The error for the values ranges between 10% to 20%. This may be due to the parallax error while reading the values and also the own-constructed manometer was not that well-constructed. Water can be trapped at the tube of the manometer and this will reduce the sensitivity of the reading. Thus, the measurements were done several times to obtain a better and more accurate measurement. From the results, it can be said that the pressure drop of Helix Prime is describable using Ergun's equation with desirable certainty.

From equation (20),

$$\frac{\Delta p}{L} \frac{D_p}{\rho V_s^2} \left[\frac{\varepsilon^3}{(1-\varepsilon)^2} \right] \left(\frac{D_p V_s \rho}{\mu} \right) = \left[\left(\frac{D_p V_s \rho}{(1-\varepsilon)\mu} \right) \right] k_2 + k_1$$

The Ergun's constant k_2 can be compared with that from Ergun's equation of 1.75 by assuming the k_1 value in equation (20) to be 150.

$$\frac{\Delta p}{L} \frac{D_p}{\rho V_s^2} \left[\frac{\varepsilon^3}{(1-\varepsilon)^2} \right] \left(\frac{D_p V_s \rho}{\mu} \right) = \left[\left(\frac{D_p V_s \rho}{(1-\varepsilon)\mu} \right) \right] k_2 + 150$$

The Y-axis or the friction factor Reynolds number can be calculated using the left-hand side correlation:

$$\frac{\Delta p}{L} \frac{D_p}{\rho V_s^2} \left[\frac{\varepsilon^3}{(1-\varepsilon)^2} \right] \left(\frac{D_p V_s \rho}{\mu} \right)$$

The X-axis of the Reynolds number can be calculated using the right-hand side correlation:

$$\left(\frac{D_p V_s \rho}{(1-\varepsilon)\mu} \right)$$

With all the values obtained for the X and Y axis and also by assuming the k_1 value to be 150, the graph of Friction Reynolds number against Reynolds number is plotted as shown:

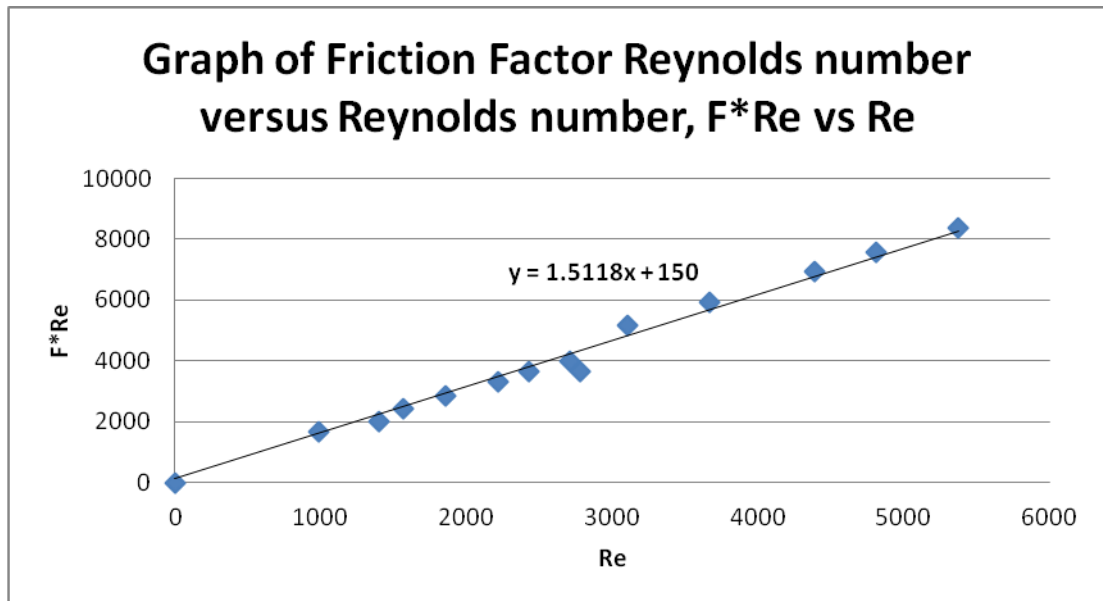


Figure 16: Graph of Friction Factor Reynolds number versus Reynolds number of Helix Prime

From **Figure 16**, the Ergun's constant k_2 obtained from the experiment is 1.5118. Taken the fact that we included the effects of the packing column surface area in our calculation (where Ergun's equation did not take into account), the obtained k_2 value for Helix Prime is reliable and comparable with the Ergun's equation as it is within the range of 1.5 to 1.8.

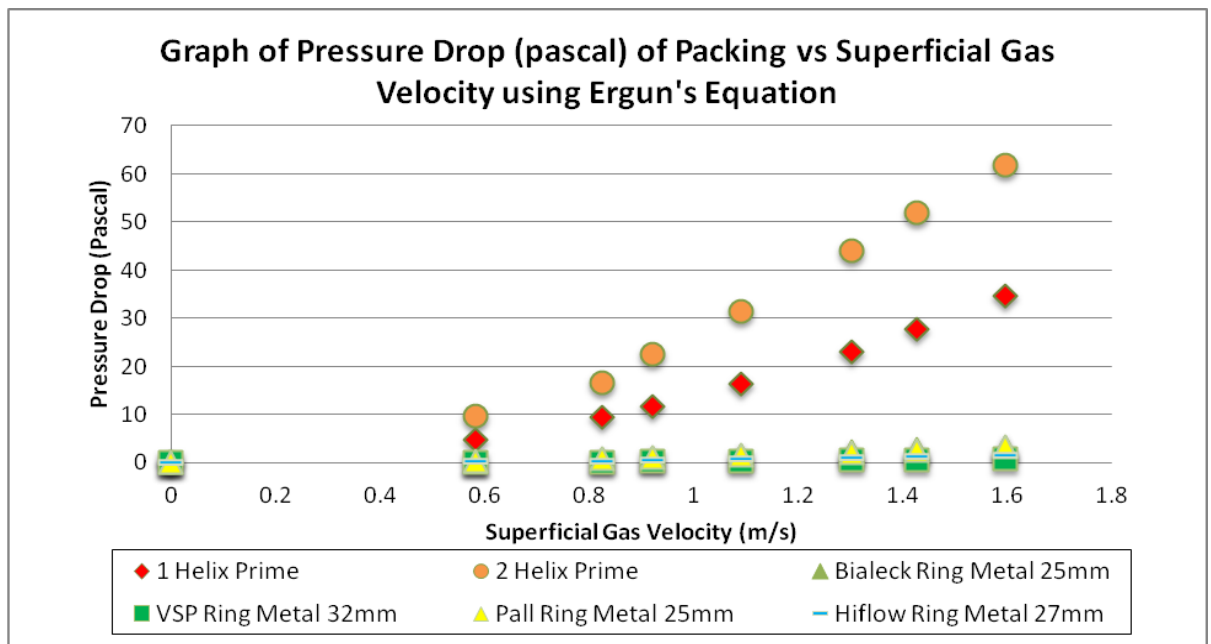


Figure 17: Graph of Pressure Drop of Packing versus Superficial Gas Velocity for different packing.

From **Figure 17**, the pressure drop for one unit and two units of Helix Prime increases exponentially as the superficial gas velocity increases. For one unit of Helix Prime, the highest pressure drop was 35 Pascal at the superficial velocity of 1.6 m/s. The pressure drop for two units of Helix Prime was roughly double of this value at the same velocity. This is because the surface area and volume of two units of Helix Prime are almost double of that of one unit of Helix Prime. Both these results show that the pressure drop of Helix Prime is a higher than the other packing elements. This is because the equivalent spherical diameter of Helix Prime is very small. It almost 18 times smaller than Bialacki Ring Metal 25mm and Pall Ring Metal 25mm, which have the smaller equivalent spherical diameters amongst the four packing elements found in the industry. The maximum acceptable pressure drop in packed bed for absorber and stripper application is 100Pascal per meter of packed bed (Mackowiak, 2010). Even though the pressure drop performance of Helix Prime is inferior as compared to the other packing elements in the industry, it is still in the acceptable range to be applied in the industry.

4.3 MASS TRANSFER EFFICIENCY

The mass transfer efficiency of Helix Prime can be evaluated using the mathematical model and correlations developed by Higbie (1935), Mackowiak (2011), and Schultes (2011), which comprises of equation from (3) to (15).

By selecting an absorption system conducted by Mackowiak (2011), we can obtain the necessary constants required for the above correlations to evaluate the performance of Helix Prime with respect to the specific liquid load, u_L of the system. The conditions of the absorption system from the work of Mackowiak (2011) are as followed:

- System: CO₂ – water / Air
- Pressure: 1.0 bar
- Liquid Temperature: 295.5 K
- Gas Capacity Factor, F_v : $0.96 \text{ kg}^{\frac{1}{2}} / \text{m}^{\frac{1}{2}} \text{ s}$
- Gravity Acceleration: $9.81 \text{ m} / \text{s}^2$
- Surface Tension of Water: $0.07275 \text{ kg} / \text{s}^2$
- Kinematic Viscosity of Water: $0.000000961 \text{ m}^2 / \text{s}$
- Diffusion Coefficient: $0.0000000016 \text{ m}^2 / \text{s}$

The differential density, $\Delta\rho$, can be obtained from the work of Mackowiak (2011) by using equation (14) and (15). This constant depends on the concentration of carbon dioxide in the air of the system.

The absorption system selected from Mackowiak's work is based on the experimental results from the Pall Ring Metal 25mm. The characteristics of this packing element are as below:

- Geometric surface area per unit volume, $a \text{ (} \frac{\text{m}^2}{\text{m}^3} \text{)} = 232.1$
- Form factor, $\phi_p = 0.28$
- Void fraction, $\varepsilon = 0.941$

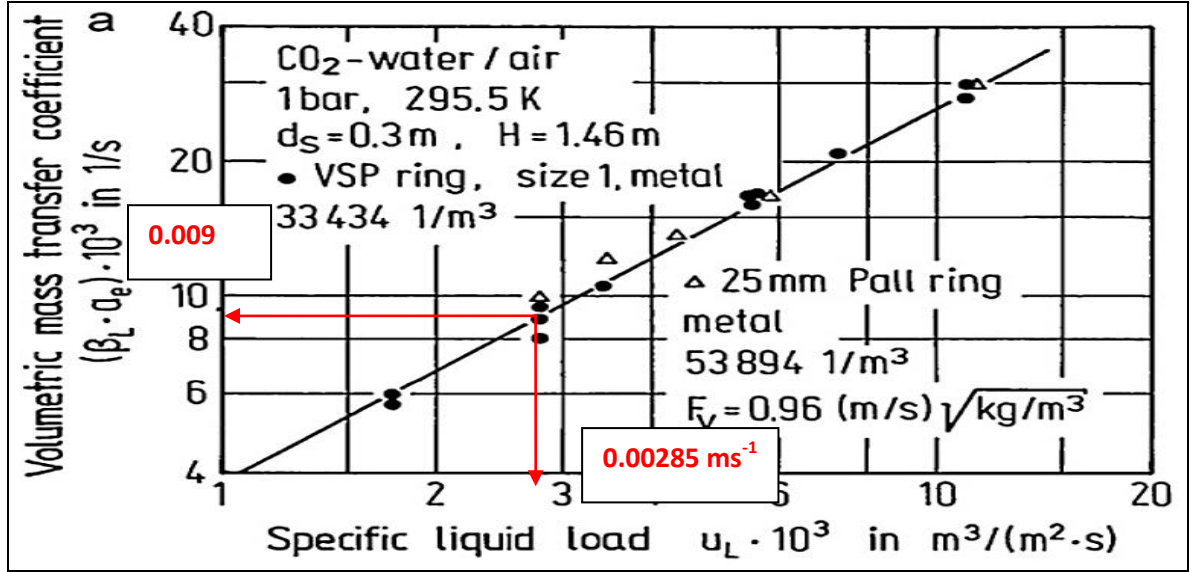


Figure 18: Experimental data for volumetric mass transfer coefficient, $\beta_L a_e$, as a function of specific liquid load, μ_L (Mackowiak, 2013).

From **Figure 18**, the specific liquid loading, u_L obtained is 0.00285 and this value is substituted into equation (4) to calculate the Reynolds number and then determine the formula for volumetric mass transfer coefficient to be used, $\beta_L a_e$.

$$Re_L = \frac{\mu_L}{a \cdot v_L} = \frac{0.00285 \text{ ms}^{-1}}{232.1 \text{ m}^{-1} \times (0.961 \times 10^{-6} \text{ m}^2 \text{ s}^{-1})} = 12.778$$

Reynolds number, $Re > 2.0$. Equation (14) is used to find the differential density, $\Delta\rho$.

Hydraulic diameter, d_h is calculated using equation (12).

$$d_h = \frac{4\varepsilon}{a} = \frac{4 \times 0.942}{232.1 \text{ m}^{-1}} = 0.0162 \text{ m}$$

With all the values and constants obtained, we can now calculate the differential density with equation (14).

$$\beta_L a_e = \frac{15.1}{(1 - \phi_p)^{1/3} d_h^{1/4}} \left(\frac{D_L \Delta\rho g}{\sigma_L} \right)^{1/2} \left(\frac{a}{g} \right)^{1/6} u_L^{5/6}$$

$$0.009 = \frac{15.1 \times (0.00285 \text{ ms}^{-1})^{5/6}}{(1 - 0.28)^{1/3} \cdot (0.0162 \text{ m})^{1/4}} \left[\frac{(1.6 \times 10^{-9} \text{ m}^2 \cdot \text{s}^{-1}) \cdot (9.81 \text{ m} \cdot \text{s}^{-2}) \cdot \Delta\rho}{0.07275 \text{ kg} \cdot \text{s}^{-2}} \right]^{1/2} \cdot \left(\frac{232.1 \text{ m}^{-1}}{9.81 \text{ m} \cdot \text{s}^{-2}} \right)^{1/6}$$

$$\Delta\rho = 1023.633 \text{ kg} \cdot \text{m}^{-3}$$

By having all the constants for the mathematical model developed by Higbie (1935), Mackowiak (2011), and Schultes (2011), we can compare the performance of Helix Prime analytically with the other existing packing elements. Figure 5.1 shows the comparison of effective interfacial area of mass transfer per unit volume plotted against the specific liquid load for one unit of Helix Prime, two units of Helix Prime, Bialecki Ring Metal 25mm, VSP Ring Metal 32mm, Pall Ring metal 25mm and Hiflow Metal 27mm.

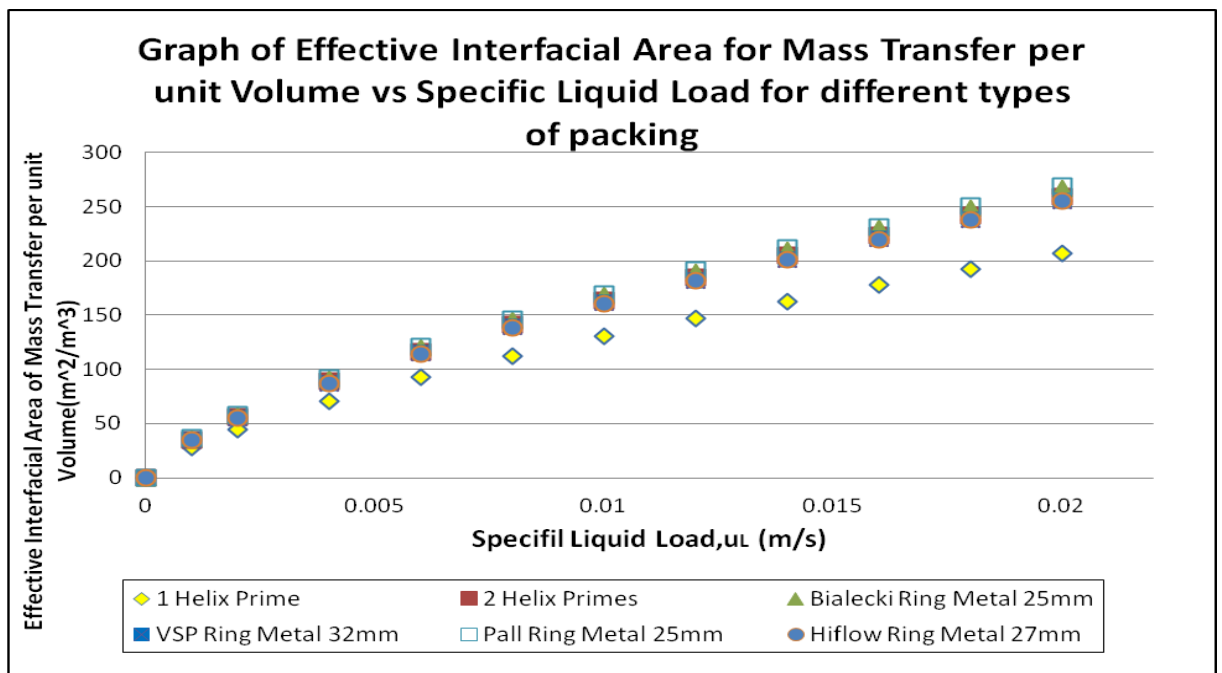


Figure 19: Graph of effective interfacial area for mass transfer per unit volume versus specific liquid load for different types of packing elements.

The results obtained from **Figure 19** is calculated using equation (3) to (7), in which the effective interfacial area for mass transfer per unit volume is directly proportional to the geometric surface area of the packing. Since one unit of Helix Prime has a smaller geometric surface area as compared to the other packing elements including two units of Helix Prime, therefore, its effective interfacial area for mass transfer at varying specific liquid loading is lower than the others. The scenario is different when two units of Helix Prime is used, the results showed that it has a comparable effective mass transfer per unit volume with the other packing elements.

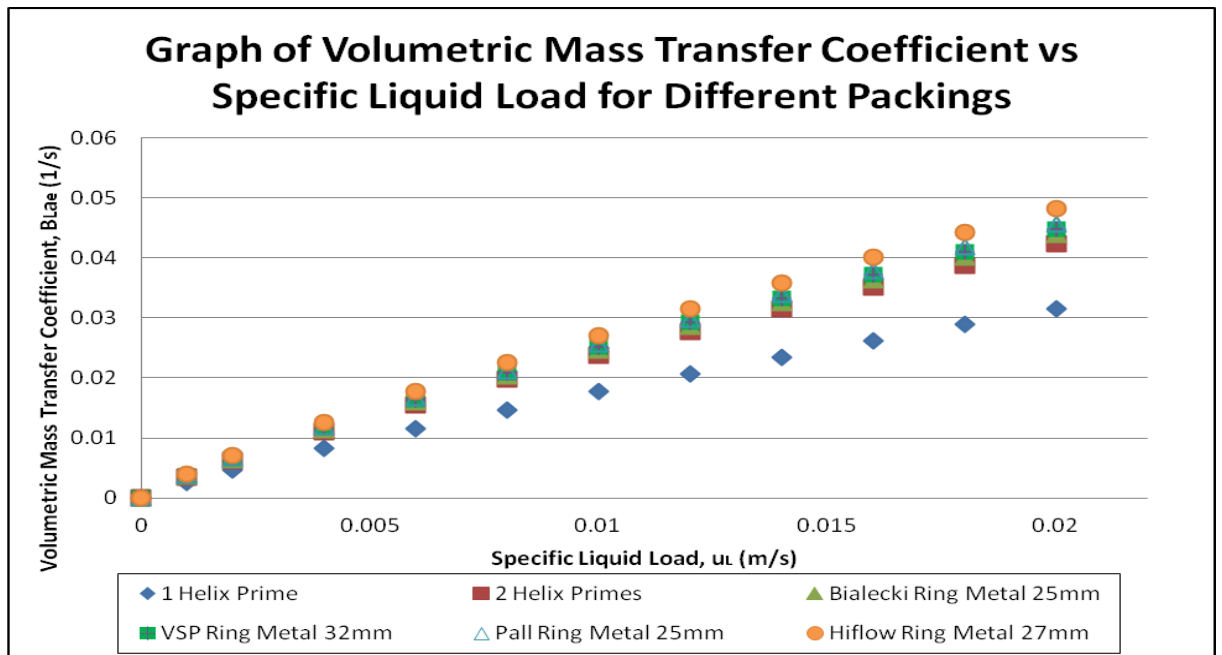


Figure 20: Graph of volumetric mass transfer coefficient versus specific liquid load for different types of packing elements.

Figure 20 shows the comparison of the volumetric mass transfer coefficient plotted against the specific liquid load for one unit of Helix Prime, two Units of Helix Prime, Bialecki Ring Metal 25mm, VSP Ring Metal 32mm, Pall Ring Metal 25mm and Hiflow Ring Metal 27mm. With the help of equation (14), the volumetric of mass transfer coefficient of the respective packing elements are calculated and compared. The results obtained shows that the volumetric mass transfer coefficient for two units of Helix Prime is comparable with those from the industry. Although two units of Helix Prime shows positive results, one unit of Helix Prime is inferior to the other packing because its effective interfacial area for mass transfer and its geometric surface area per packing are relatively small when compared with the others.

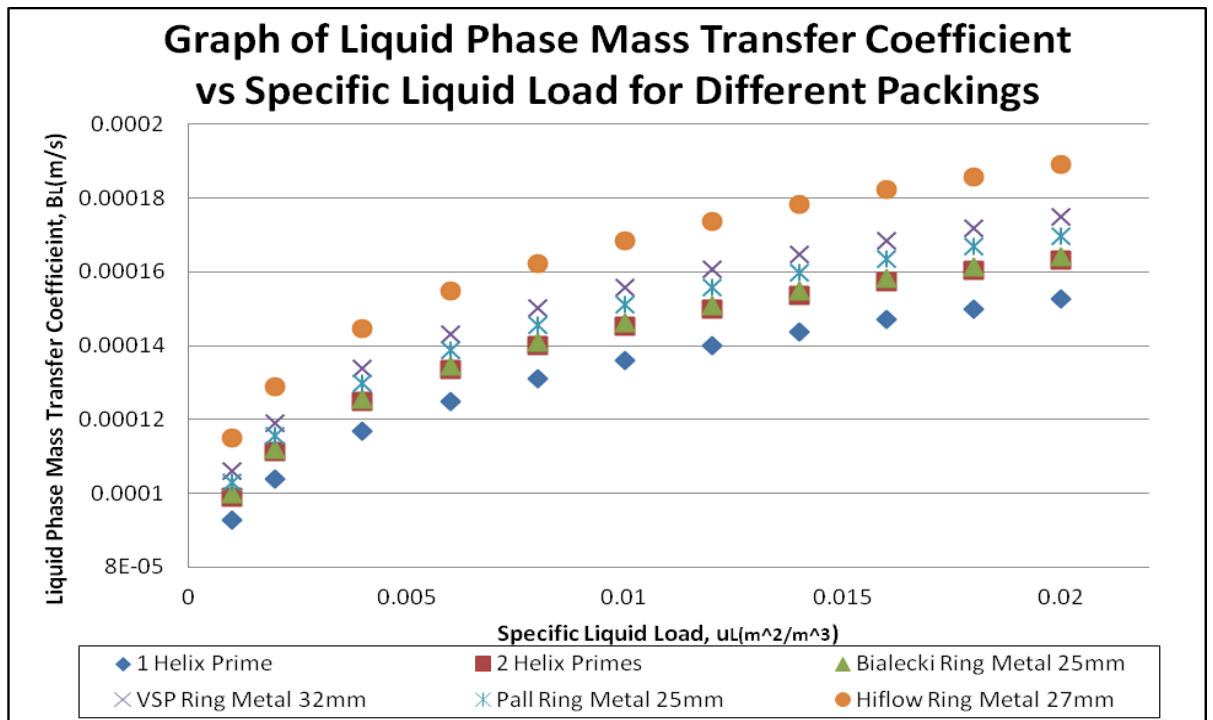


Figure 21: Graph of liquid phase mass transfer coefficient versus specific liquid load for different types of packing elements.

Figure 21 shows the comparison of the liquid phase mass transfer coefficient plotted against the specific liquid load for one unit of Helix Prime, two Units of Helix Prime, Bialecki Ring Metal 25mm, VSP Ring Metal 32mm, Pall Ring Metal 25mm and Hiflow Ring Metal 27mm. One unit of Helix Prime has the lowest liquid phase mass transfer coefficient when compared with the others. This result differs when two units of Helix Prime is used. The mass transfer coefficient obtained for two units of Helix Prime is comparable with the other packing elements due to its large geometric surface area per packing.

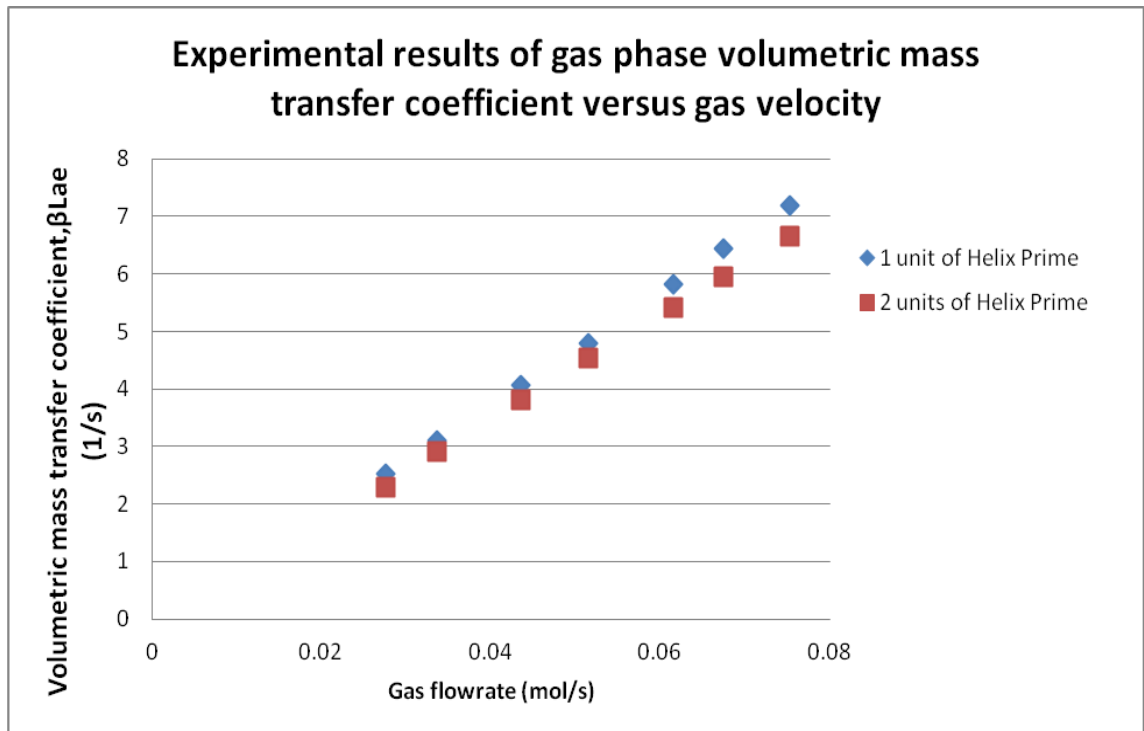


Figure 22: Graph of experimental results of liquid phase mass transfer coefficient versus gas flow rate at fixed water flow rate of 0.022 m/s

Figure 22 shows the experimental results of the gas phase volumetric mass transfer coefficient, K_{ga} obtained at a fixed water flow rate of 0.22m/s. The gas flow rate is being manipulated in this study. It is observed that the volumetric mass transfer coefficient for a single unit of Helix Prime is slightly higher than that of two units. A reason that might explain this phenomenon is that the experiment was conducted at different days, in which the moisture content of air differs from each other. Besides, the two units in parallel might reduce the vibration of the springs when fluids are moving through it. This in-turn reduces the mass transfer of the moisture. Comparing our findings with the work of Grunig et. al. (2012) in ‘Mass transfer characteristics of liquid film flowing down a vertical wire in a counter current gas flow’, we found that the volumetric mass transfer coefficients for one unit and 2 units are approximately 10 times the ones obtained by Grunig (2012). A factor that might explain this variation is Helix Prime uses around 4 m of wire as compared to 1 m used in Grunig’s work; a longer wire coiled to a spring shape gives more surface area for the mass transfer to occur and thus higher mass transfer coefficient. This is an interesting finding and further experiments need to be conducted in the future.

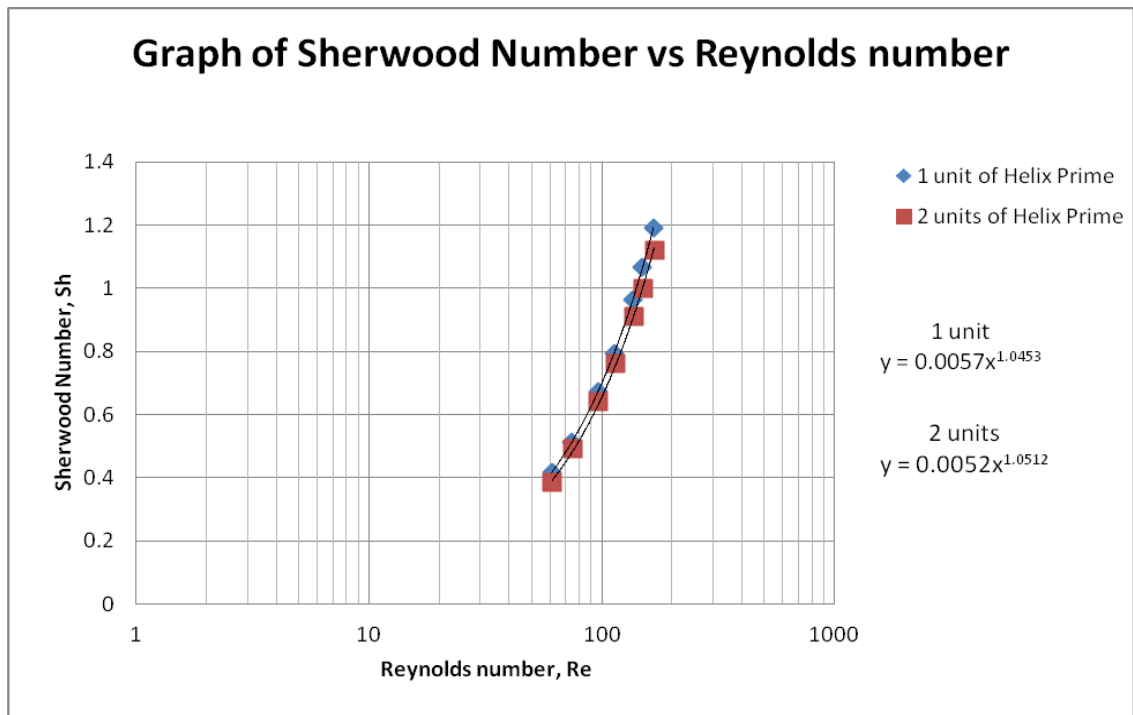


Figure 23: Graph of experimental results of Sherwood number versus Reynolds number at fixed water flow rate of 0.022 m/s

From **Figure 23**, we obtained a graph of Sherwood number versus the Reynolds number for the Helix Prime at a fixed water flow rate of 0.022 m/s. Sherwood number is a function volumetric mass transfer coefficient. Since the 1 unit of Helix Prime has a higher volumetric mass transfer coefficient, the Sherwood number of it will be slightly higher than that of the 2 units. The Sherwood number obtained from this study with regards to the Reynolds number is approximately the same as the work of Grunig et. al. (2012). This gives a positive finding to further the study in order to improve the mass transfer of future packing elements.

CHAPTER 5

CONCLUSION AND RECOMMENDATION

5.1 CONCLUSION

As a conclusion, the new packing element, Helix Prime, is a new and innovative idea that shows a promising breakthrough in the development of random packing elements. It has the rigid structure of the older generation packing elements and the flexible structure of the newer generation of packing elements. Therefore, it overcomes the drawbacks of both previous and new generation of packing elements. It has a high mass transfer area with high structural strength for operation. The packing characteristics of Helix Prime are comparable with the other packing elements in terms of void fraction and geometric surface area per unit volume when two units are bind together in parallel.

The pressure drop across the packed bed for Helix Prime is higher than the other packing element used in the research. When two units of Helix Prime are used, the pressure drop is almost double than that when one unit of Helix Prime is used. Although Helix Prime is inferior in terms of pressure drop, the pressure drop is still within an acceptable range that can be applied in the absorption and stripper application.

In terms of the mass transfer performance, one unit of Helix Prime is inferior to the other packing elements. It has a lower effective interfacial area for mass transfer, a lower volumetric mass transfer coefficient and also a lower liquid phase mass transfer coefficient when compared with the other packing elements. But the results of the two unit of Helix Prime show promising results for our work. It has a comparable effective interfacial area for mass transfer, volumetric mass transfer coefficient and liquid phase mass transfer coefficient with the other packing elements.

Based on the results, Helix Prime is a new type of packing element that is comparable with other packing elements used in the industry. The pressure drop and mass transfer performance of Helix Prime is within the satisfactory range applied in the industry. Besides, with this design, Helix Prime can be easily taken out for cleaning, this will reduce the cleaning time of the packed bed column. Helix Prime has met the research's objectives and has proven itself to be worthy of future extension work in order to design a better packing element that can excel the current packing elements for higher mass transfer. With time, I believe that this type of packing element can be an evolutionary idea to create a better packing element in industry.

5.2 SUGGESTED FUTURE WORK FOR EXPANSION AND CONTINUATION

From this work, there are improvements to be done on the experiments to obtain better results.

First of all, the manometer should be reconstructed with a better material and calibrated properly so that it is more sensitive to pressure changes. The fittings of the manometer should be slightly covered so that water will not flow into the manometer.

Thermocouples can be put into the water inlet and outlet stream to measure the temperature of the water and seek any changes in it. The column can be made from transparent material so that any observation in the packing column is made possible. More units of Helix Prime can be used to increase the mass transfer area per unit volume of the packing.

The diameter of Helix Prime can be increased and wicks can be placed on it to increase the wettability and also mass transfer. Layers upon layers of spring are also an interesting topic for the future research work.

REFERENCE

1. Ergun, S. (1952). Fluid Flow through Packed Column. Chem. Eng. Prog. 48.
2. Geankoplis, C.J. (2003). Transport Phenomena and Separation Process Principles: Includes Unit Operation: Prentice Hall Professional Technical Reference.
3. Grunig, J., Lyagin, E., Horn, S., Skale, T., Kraume, M. (2012) Mass Transfer Characteristics of Liquid Films Flowing Down a Vertical Wire in a Counter Current Gas Flow. Chemical Engineering Science: 69 (2012) 329-339.
4. Hansen, A.T., Hondzo, M., & Hurd, C.L. (2011). Photosynthetic Oxygen Flux by *Macrocyctis pyrifera*: A Mass Transfer Model with Experimental Validation. Marine Ecology Progress Series. Vol. 434: 45-55.
5. Koretsky, M.D. (2004). Engineering and Chemical Thermodynamics. John Wiley & Sons.
6. Lee, K.R., & Hwang, S.T. (1989). Gas Absorption with Wetted-Wick Column. Korean J. of Chem. Eng., 6(3) 259-269.
7. Maćkowiak, J. (2011). Model for the Prediction of Liquid Phase Mass Transfer Of Random Packed Columns For Gas-Liquid Systems: Chemical Engineering Research and Design, 89 (2011), 1308-1320.
8. Maćkowiak, J. (2010). Fluid Dynamics of Packed Columns: Principles Of The Fluid Dynamic Design Of Columns For Gas/Liquid Liquid/Liquid Systems. Springer Berlin Heidelberg.
9. Schultes, M. (2003). RASCHIG SUPER-RING- A New Fourth Generation Packing Offers New Advantages: Tans ICheme, Vol 81, Part A.
10. Subbarao, D., Rosli, F.A., Azmi, F.D., Manogaran, P., & Mahadzir, S. (2013). A Rivulet Flow Model for Wetting Efficiency in A Packed Bed. AiChe Spring Meeting, San Antonio, Texas, USA.
11. Subramanian, R.S., (n.d.). Flow through Packed Beds and Fluidized Beds. [Online]

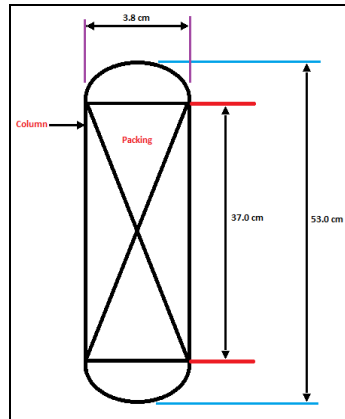
Available:

<http://web2.clarkson.edu/projects/subramanian/ch301/notes/packfluidbed.pdf>

APPENDICES

Appendix A (Packing column and packing element characteristics and dimensions)

Example calculation of the dimension of packing column



Diameter, $D = 3.8 \text{ cm} = 0.038\text{m}$

$R = 0.019\text{m}$

Height, $H = 37 \text{ cm} = 0.37 \text{ m}$

$$\begin{aligned} \text{Cross sectional area of column, } A_c &= \pi \left(\frac{D}{4} \right)^2 \\ &= \pi \left(\frac{0.038}{4} \right)^2 \\ &= 0.001134\text{m}^2 \end{aligned}$$

$$\begin{aligned} \text{Surface area of column, } A_s &= 2\pi RH \\ &= 2 \times \pi \times 0.019 \times 0.37\text{m}^2 \\ &= 0.04417\text{m}^2 \end{aligned}$$

$$\begin{aligned} \text{Volumn of column, } V_c &= \pi R^2 H \\ &= \pi \times 0.019^2 \times 0.37\text{m}^3 \\ &= 4.196 \times 10^{-4} \text{m}^3 \end{aligned}$$

Example calculation of the characteristics and properties of Helix Prime (spring and rod)

Spring

$$\text{Helix Diameter, } D = 2.3 \text{ cm} = 0.023 \text{ m} \quad R = 0.0115 \text{ m}$$

$$\text{Wire diameter, } d = 0.1 \text{ cm} = 0.001 \text{ m} \quad r = 0.0005 \text{ m}$$

$$\text{Height of Helix, } H = 33 \text{ cm} = 0.33 \text{ m}$$

$$\text{Number of loops, } n = 60$$

$$\begin{aligned} \text{Length of the spring} &= 2n\pi R \\ &= 2 \times 60 \times \pi \times 0.0115 \text{ m} \\ &= 4.335 \text{ m} \end{aligned}$$

$$\begin{aligned} \text{Surface Area of spring} &= 2\pi r L \\ &= 2 \times \pi \times 0.0005 \times 4.335 \text{ m}^2 \\ &= 0.0136 \text{ m}^2 \end{aligned}$$

$$\begin{aligned} \text{Volume of spring} &= \pi r^2 (2n\pi R) \\ &= \pi \times 0.0005^2 \times 2 \times 60 \times \pi \times 0.0115 \text{ m}^3 \\ &= 3.405 \times 10^{-6} \text{ m}^3 \end{aligned}$$

Rod

$$\text{Rod Length} = 34 \text{ cm} = 0.34 \text{ m}$$

$$\text{Rod dimension} = 0.5 \text{ cm} \times 0.7 \text{ cm} = 0.005 \text{ m} \times 0.007 \text{ m}$$

$$\begin{aligned} \text{Surface area of rod} &= 2(0.005 \times 0.007) + 2(0.005 \times 0.34) + 2(0.007 \times 0.34) \text{ m}^2 \\ &= 8.23 \times 10^{-3} \text{ m}^2 \end{aligned}$$

$$\begin{aligned} \text{Volume of rod} &= 0.004 \times 0.007 \times 0.34 \text{ m}^3 \\ &= 1.19 \times 10^{-5} \text{ m}^3 \end{aligned}$$

$$\begin{aligned} \text{Total surface area, SA} &= 0.04417 + 0.0136 + 8.23 \times 10^{-3} m^2 \\ &= 0.04428 m^2 \end{aligned}$$

$$\begin{aligned} \text{Total Volume, VP} &= 1.19 \times 10^{-5} + 3.405 \times 10^{-6} m^3 \\ &= 1.5305 \times 10^{-5} m^3 \end{aligned}$$

$$\begin{aligned} \text{Geometric surface area per unit volume, } \alpha &= \frac{SA}{V_c} \\ &= \frac{0.04428}{4.196 \times 10^{-4}} \\ &= 105.53 m^2 / m^3 \end{aligned}$$

$$\begin{aligned} \text{Void fraction, } \varepsilon &= \frac{V_c - VP}{V_c} \\ &= \frac{4.196 \times 10^{-4} - 1.5305 \times 10^{-5}}{4.196 \times 10^{-4}} \\ &= 0.9635 \end{aligned}$$

$$\begin{aligned} \text{Equivalent spherical diameter, } D_p &= \frac{6VP}{SA} \\ &= \frac{6 \times 1.5305 \times 10^{-5}}{0.04428} m \\ &= 2.074 \times 10^{-3} m \end{aligned}$$

Appendix B (Pressure drop)

Example calculation of orifice air flow rate

Pipe diameter, $D_i = 3.8$ cm

Orifice diameter, $D_o = 1.3$ cm

Orifice pressure difference in water height = 0.4 cm

Flow coefficient, $C_f = 0.61$

Inlet air Dry-bulb temperature = 16.0°C

Inlet air Wet-bulb temperature = 13.6°C

Density of Water = 1000.0 kg/m³

The orifice pressure difference is calculated by:

$$\Delta p = \rho g h = (1000.0 \text{ kg/m}^3) \cdot (9.81 \text{ m/s}^2) \cdot (0.004 \text{ m}) = 39.24 \text{ kg/m} \cdot \text{s}^2 = 39.24 \text{ Pa}$$

The area of the orifice, A_o , is:

$$A_o = \pi r^2 = \pi \frac{(0.013 \text{ m})^2}{4} = 0.000133 \text{ m}^2$$

Based on the dry-bulb and wet-bulb temperature of the inlet air, the density of inlet air can be found in the psychometric chart.

$$\rho_{\text{air}} = 1.1725 \text{ kg/m}^3$$

Substituting all the constants into equation (21), the volumetric flow rate of air can be calculated:

$$Q_{\text{volume}} = C_f A_o \sqrt{\frac{2\Delta p}{\rho}} = (0.61) \cdot (0.000133 \text{ m}^2) \cdot \sqrt{\frac{2(39.24 \text{ kg/m} \cdot \text{s}^2)}{1.1725 \text{ kg/m}^3}} = 0.0006623 \text{ m}^3 / \text{s}$$

The mass flow rate can be calculated by multiplying the volumetric flow rate with density:

$$Q_{mass} = (0.0006623 \text{ m}^3 / \text{s})(1.1725 \text{ kg} / \text{m}^3) = 0.0007765 \text{ kg} / \text{s}$$

The superficial gas velocity with respect to column cross-sectional area is calculated by dividing volumetric flow rate with column cross-sectional area:

$$V_s = (0.0006623 \text{ m}^3 / \text{s}) / (0.001134 \text{ m}^2) = 0.584 \text{ m} / \text{s}$$

Example calculation of Ergun's pressure drop using 1 unit of Helix Prime

Void fraction, $\varepsilon = 0.9635$

Superficial Gas Velocity, $V_s = 0.584 \text{ m/s}$

Air density, $\rho = 1.1725 \text{ kg/m}^3$

Air dynamic viscosity, $\mu = 0.00001983 \text{ kg/m.s}$

Equivalent spherical diameter of packing, $D_p = 0.002074 \text{ m}$

Length of packing in the column, $L = 0.33 \text{ m}$

By assuming $k_1=150$ and $k_2 = 1.75$, rearrange Ergun's equation to get the pressure drop on the left-hand side of the equation:

$$\Delta p = \frac{150(1-\varepsilon)^2 \mu V_s L}{D_p^2 \varepsilon^3} + \frac{1.75 \rho V_s^2 L (1-\varepsilon)}{D_p \varepsilon^3} \quad [kg / m.s]$$

Substitute the constants value into the equation to calculate the pressure drop in Pascal:

$$\Delta p = \frac{150(1 - 0.9635)^2(0.00001983 \text{ kg/m.s})(0.584 \text{ m/s})(0.33 \text{ m})}{(0.002074 \text{ m})^2(0.9635)^3} +$$

$$\frac{1.75(1.1725 \text{ kg/m}^3)(0.584 \text{ m/s})^2(0.33 \text{ m})(1 - 0.9635)}{(0.002074 \text{ m})(0.9635)^3}$$

$$= 0.198 + 4.544$$

$$= 4.742 \text{ kg/m.s} = 4.742 \text{ Pa}$$

Example of calculation for Ergun's Constant using 1 unit of Helix Prime

Pressure drop = 0.981 kg/m.s^2

Void fraction, $\varepsilon = 0.9635$

Superficial Gas Velocity, $V_s = 0584 \text{ m/s}$

Air density, $\rho = 1.1725 \text{ kg/m}^3$

Air dynamic viscosity, $\mu = 0.00001983 \text{ kg/m.s}$

Equivalent spherical diameter of packing, $D_p = 0.002074 \text{ m}$

Length of packing in the column, $L = 0.33 \text{ m}$

The modified Ergun's equation is:

$$\frac{\Delta p}{L} \frac{D_p}{\rho V_s^2} \left(\frac{\varepsilon^3}{1-\varepsilon} \right) \left(\frac{D_p V_s \rho}{(1-\varepsilon)\mu} \right) = \left(\frac{D_p V_s \rho}{(1-\varepsilon)\mu} \right) k_2 + k_1$$

The value for k_1 is assumed to be 150.

The value for Y-axis is calculated as follows:

$$\begin{aligned} & \frac{\Delta p}{L} \frac{D_p}{\rho V_s^2} \left(\frac{\varepsilon^3}{1-\varepsilon} \right) \left(\frac{D_p V_s \rho}{(1-\varepsilon)\mu} \right) \\ &= \frac{0.981 \text{ kg/m.s}^2}{0.33 \text{ m}} \frac{0.002074 \text{ m}}{(1.1725 \text{ kg/m}^3)(0.584 \text{ m/s})^2} \left(\frac{0.9635^3}{1-0.9635} \right) \left(\frac{(0.002074 \text{ m})(0.584 \text{ m/s})(1.1725 \text{ kg/m}^3)}{(1-0.9635)(0.00001983 \text{ kg/m.s})} \right) \\ &= 741.32 \end{aligned}$$

The value for X-axis is calculated as follows:

$$\begin{aligned} & \left(\frac{D_p V_s \rho}{(1-\varepsilon)\mu} \right) \\ &= \frac{(0.002074 \text{ m})(0.584 \text{ m/s})(1.1725 \text{ kg/m}^3)}{(1-0.9635)(0.00001983 \text{ kg/m.s})} \\ &= 1962.06 \end{aligned}$$

The value for k_1 is assumed to be 150.

When all the values for X-axis and Y-axis have been calculated at specified superficial gas velocity, a graph of Y-axis vs X-axis is plotted for every specific liquid load. The gradient value represents the value for constant k_2 .

Appendix C (Mass transfer)

Example of calculation for moisture content using 1 unit of Helix Prime

Inlet gas relative humidity, RH (%) = 22.22

Outlet gas relative humidity, RH (%) = 100

Inlet gas dry-bulb temperature (°C) = 26.0

Outlet gas dry-bulb temperature (°C) = 27.1

Volumetric flow rate of air, $Q_{volume} = 0.0006623$

1 mol of air occupies 0.0224 m³ of air

Total pressure of the system is 101.3 kPa

Based on the inlet gas dry-bulb temperature, we can obtain the partial pressure of air in the inlet gas from the steam table (Appendix D).

$$P^* = 3.3845 \text{ kPa}$$

To calculate the partial pressure of water in the inlet air, we can use the following formula:

$$\begin{aligned} P_{H_2O} &= P^* \times \frac{RH}{100\%} \\ &= 3.3845 \times \frac{22.22}{100} \\ &= 0.7520 \text{ kPa} \end{aligned}$$

The mol fraction of water in the inlet gas can be obtained by:

$$\begin{aligned}y_{H_2O}^{in} &= \frac{P_{H_2O}}{P_{total}} \\ &= \frac{0.7520}{101.3} \\ &= 0.007424\end{aligned}$$

By repeating the same steps for the outlet gas dry-bulb temperature, we can obtain the mol fraction of water in the outlet gas.

$$y_{H_2O}^{out} = 0.03575$$

The moisture content of the gas flowing through the column can be calculated as follow:

$$\begin{aligned}\text{Molar flow rate of air} &= Q_{volume} \times \frac{1 \text{ mol}}{0.0224 \text{ m}^3} \\ &= 0.0006623 \times \frac{1}{0.0224} \\ &= 0.0295 \text{ mol/s}\end{aligned}$$

$$\begin{aligned}\text{Moisture content} &= \text{Molar flow rate} \times (y_{H_2O}^{out} - y_{H_2O}^{in}) \\ &= 0.0295 \times (0.03575 - 0.007424) \\ &= 0.000835 \text{ mol/s}\end{aligned}$$

Example of calculation for effective interfacial area for mass transfer using 1 unit of Helix Prime

Void fraction, $\varepsilon = 0.9635$

Geometric surface area per unit volume ($\frac{m^2}{m^3}$) = 105.53

Form factor, $\varphi_p = 0.208$

Gravitational acceleration, $g = 9.81 \text{ m/s}^2$

Surface tension, $\sigma_L = 0.07275 \text{ kg/s}^2$

$\Delta\rho = 1023.633 \text{ kg/m}^3$

Assuming specific liquid loading, $u_L = 0.001 \text{ m/s}$

Equation (7) is used to calculate the mean droplet diameter, d_t :

$$\begin{aligned}d_t &= \sqrt{\frac{\sigma_L}{\Delta\rho g}} \\&= \sqrt{\frac{0.07275}{1023.633 \times 9.81}} \\&= 0.00269 \text{ m}\end{aligned}$$

Equation (5) is used calculate the specific liquid hold-up, h_L :

$$\begin{aligned}h_L &= 0.57 \left(\frac{u_L^2 \times a}{g} \right)^{1/3} \\&= 0.57 \left(\frac{0.001^2 \times 105.53}{9.81} \right)^{1/3}\end{aligned}$$

$$= 0.012583 \text{ m}^2/\text{m}^3$$

With all these values, we can calculate the effective interfacial area for mass transfer at the specific liquid loading of 0.001 m/s from equation (3)

$$\begin{aligned} a_e &= 6 \frac{h_L}{d_t} \\ &= 6 \left(\frac{0.012583}{0.00269} \right) \\ &= 28.05 \text{ m}^2/\text{m}^3 \end{aligned}$$

By varying the specific liquid load for the system, we can calculate the effective interfacial area to plot the graph.

By changing the characteristics of the packing, we can also calculate the effective interfacial area for different packing elements.

**Example of calculation for volumetric mass transfer coefficient, $\beta_{L,ae}$
using 1 unit of Helix Prime**

Void fraction, $\varepsilon = 0.9635$

Geometric surface area per unit volume (m^2/m^3) = 105.53

Form factor, $\varphi p = 0.208$

Gravitational acceleration, $g = 9.81 \text{ m/s}^2$

Surface tension, $\sigma_L = 0.07275 \text{ kg/s}^2$

$\Delta\rho = 1023.633 \text{ kg/m}^3$

Diffusion coefficient, $D_L = 1.6 \times 10^{-9} \text{ m}^2 / \text{s}$

Assuming specific liquid loading, $u_L = 0.001 \text{ m/s}$

Using equation (13), we can calculate the hydraulic diameter, d_h

$$\begin{aligned}d_h &= \frac{4\varepsilon}{a} \\ &= \frac{4 \times 0.9635}{105.53} \\ &= 0.03652 \text{ m}\end{aligned}$$

By checking with equation (4), the Reynolds number obtained was greater than 2. Thus, equation (14) is to be used:

$$\beta_L a_e = \frac{15.1}{(1-\phi_p)^{1/3} d_h^{1/4}} \left(\frac{D_L \Delta \rho g}{\sigma_L} \right)^{1/2} \left(\frac{a}{g} \right)^{1/6} u_L^{5/6}$$

$$\beta_L a_e = \frac{15.1}{(1-\phi_p)^{1/3} d_h^{1/4}} \left(\frac{D_L \Delta \rho g}{\sigma_L} \right)^{1/2} \left(\frac{a}{g} \right)^{1/6} u_L^{5/6}$$

$$= \frac{15.1}{(1-0.208)^{1/3} 0.03652^{1/4}} \left(\frac{1.6 \times 10^{-9} \times 1023.633 \times 9.81}{0.07275} \right)^{1/2} \left(\frac{105.53}{9.81} \right)^{1/6} (0.001)^{5/6}$$

$$= 0.002607 s^{-1}$$

By varying the specific liquid load for the system, we can calculate the effective interfacial area to plot the graph.

By changing the characteristics of the packing, we can also calculate the hydraulic diameter and volumetric mass transfer coefficient for different packing elements.

**Example of calculation for liquid phase mass transfer coefficient, β_L ,
using 1 unit of Helix Prime**

We can calculate the liquid phase mass transfer coefficient by sampling dividing the volumetric mass transfer coefficient with the effective interfacial area that was calculated before.

$$\beta_L \times a_e = \beta_L a_e$$

$$\beta_L = \frac{\beta_L a_e}{a_e}$$

$$= \frac{0.002607}{28.05}$$

$$= 9.29 \times 10^{-5} \text{ m/s}$$

Example of calculation for experimental gas phase mass transfer coefficient using 1 unit of Helix Prime

Void fraction	0.9635	
Equivalent spherical diameter	2.07E-03	m
Air dynamic viscosity	1.98E-05	kg/ms
Water density	1000	kg/m ³
Cross area of column	0.001134	m ²
Flow coefficient, C_f	0.61	
Gravitational acceleration	9.81	m/s ²
Area of orifice	0.000133	m ²
Length of packing	0.33	m
Volume of column	4.20E-04	m ³
Molecular weight of air	29	g/mol
Molecular weight of water	18	g/mol
Gas constant	0.008314	m ³ kPa/K mol
Diffusion coefficient of air and water	2.60E-05	m ² /s
Density of air	1	kg/m ³

Q air (m3/s)	F air (mol/s) 1mol air =0.024m ³	Inlet gas				Y _{H2O}	Outlet gas				
		Td1	Tw1	Td1-Tw1	RH inlet gas(%)		Td2	Tw2	Td2-Tw2	RH outlet gas(%)	Y _{H2O}
0.0007	0.027529434	26	13.6	12.4	22.22	0.007423849	13.6	13.6	0	100	0.035749654
0.0008	0.033700642	26	13.6	12.4	22.22	0.007423849	13.6	13.6	0	100	0.03596229
0.0010	0.043507342	26	13.5	12.5	21.73	0.007260137	13.5	13.5	0	100	0.036174926
0.0012	0.051469475	26	13.5	12.5	21.73	0.007260137	13.5	13.5	0	100	0.03596229
0.0015	0.061510533	26.1	13.4	12.7	20.92	0.007033994	13.4	13.4	0	100	0.035749654
0.0016	0.067369487	26.1	13.3	12.8	20.43	0.00686924	13.3	13.3	0	100	0.035537019
0.0018	0.075321377	26.1	13.3	12.8	20.43	0.00686924	13.3	13.3	0	100	0.035324383

Fg*(y _{out} -y _{in}) Moisture content (mol/s)	ln (y out / y in)	K _{ga} (1/s)	Sherwood number, Sh	Velocity of air	Reynolds number
0.000779793	1.571842954	2.522248033	0.417284207	0.582633521	60.93706111
0.000961764	1.577773245	3.099303602	0.512753079	0.713241101	74.59717817
0.001258006	1.605967565	4.072683662	0.673790424	0.920790302	96.30454291
0.001477285	1.600072235	4.800325536	0.794172503	1.089301066	113.9289164
0.001766316	1.625785957	5.829002169	0.96435819	1.30181022	136.1550376
0.001931334	1.643521518	6.453866768	1.067736654	1.425809253	149.1239733
0.002143281	1.637520046	7.189293813	1.189406723	1.594103207	166.7256707

Example of calculation for experimental gas phase mass transfer coefficient using 2 units of Helix Prime

Void fraction	0.927	
Equivalent spherical diameter	2.09E-03	m
Air dynamic viscosity	1.98E-05	kg/ms
Water density	1000	kg/m ³
Cross area of column	0.001134	m ²
Flow coefficient, C_f	0.61	
Gravitational acceleration	9.81	m/s ²
Area of orifice	0.000133	m ²
Length of packing	0.33	m
Volume of column	4.20E-04	m ³
Molecular weight of air	29	g/mol
Molecular weight of water	18	g/mol
Gas constant	0.008314	m ³ kPa/K mol
Diffusion coefficient of air and water	2.60E-05	m ² /s
Density of air	1	

Q air (m3/s)	F air (mol/s)	Inlet gas				Y _{H2O}	Outlet gas				
		Td1	Tw1	Td1-Tw1	RH inlet gas(%)		Td2	Tw2	Td2-Tw2	RH outlet gas(%)	Y _{H2O}
0.0007	0.027529434	25.4	13.9	11.5	25.78	0.008284364	26.5	26.5	0	100	0.03447384
0.0008	0.033700642	25.4	13.6	11.8	24.23	0.007786273	26.5	26.5	0	100	0.03447384
0.0010	0.043507342	25.3	13.5	11.8	24.06	0.007680484	26.5	26.5	0	100	0.03447384
0.0012	0.051469475	25.3	13.4	11.9	23.55	0.007517681	26.3	26.3	0	100	0.034048569
0.0015	0.061510533	25.2	13.3	11.9	23.38	0.007413699	26.1	26.1	0	100	0.033623297
0.0016	0.067369487	25.2	13.2	12	22.87	0.00725198	25.8	25.8	0	100	0.03298539
0.0018	0.075321377	25.2	13.1	12.1	22.36	0.007090261	25.5	25.5	0	100	0.032347483

Fg*(y _{out} -y _{in}) Moisture content (mol/s)	ln (y out / y in)	K _{La} (1/s)	Sherwood number, Sh	Velocity of air	Reynolds number
0.000720981	1.425830949	2.287950777	0.38475245	0.582633521	61.43654522
0.000899388	1.487838412	2.922639843	0.491484718	0.713241101	75.20863045
0.001165708	1.501518208	3.807803351	0.640337932	0.920790302	97.09392441
0.001365531	1.510530314	4.531693684	0.7620707	1.089301066	114.86276
0.001612166	1.511889722	5.420644967	0.911560885	1.30181022	137.2710625
0.001733647	1.51479021	5.948357893	1.000303546	1.425809253	150.346301
0.001902409	1.51781404	6.663741988	1.120605865	1.594103207	168.0922746

Appendix D (Table)

Steam Table (Koretsky, 2004)

TABLE B.1 Saturated Water: Temperature Table

2

T °C	P kPa, MPa	\hat{v}_g m ³ /kg	\hat{v}_f m ³ /kg	\hat{u}_g kJ/kg	$\Delta\hat{u}_{fg}$ kJ/kg	\hat{u}_f kJ/kg	\hat{h}_g kJ/kg	$\Delta\hat{h}_{fg}$ kJ/kg	\hat{h}_f kJ/kg	\hat{s}_g kJ/kg K	$\Delta\hat{s}_{fg}$ kJ/kg K	\hat{s}_f kJ/kg K
0.01	0.6113	0.001000	206.132	0.00	2375.3	2375.3	0.00	2501.3	2501.3	0.0000	9.1562	9.1562
5	0.8721	0.001000	147.118	20.97	2361.3	2382.2	20.98	2489.6	2510.5	0.0761	8.9496	9.0257
10	1.2276	0.001000	106.377	41.99	2347.2	2389.2	41.99	2477.7	2519.7	0.1510	8.7498	8.9007
15	1.7061	0.001001	77.925	62.96	2333.1	2396.0	62.98	2465.9	2528.9	0.2245	8.5569	8.7813
20	2.3385	0.001002	57.790	83.94	2319.0	2402.9	83.94	2454.1	2538.1	0.2966	8.3706	8.6671
25	3.1691	0.001003	43.359	104.86	2304.9	2409.8	104.87	2442.3	2547.2	0.3673	8.1905	8.5579
30	4.2461	0.001004	32.893	125.77	2290.8	2416.6	125.77	2430.5	2556.2	0.4369	8.0164	8.4533
35	5.6280	0.001006	25.216	146.65	2276.7	2423.4	146.66	2418.6	2565.3	0.5052	7.8478	8.3530
40	7.3837	0.001008	19.523	167.53	2262.6	2430.1	167.54	2406.7	2574.3	0.5724	7.6845	8.2569
45	9.5934	0.001010	15.258	188.41	2248.4	2436.8	188.42	2394.8	2583.2	0.6396	7.5261	8.1647
50	12.350	0.001012	12.032	209.30	2234.2	2443.5	209.31	2382.7	2592.1	0.7037	7.3725	8.0762
55	15.758	0.001015	9.568	230.19	2219.9	2450.1	230.20	2370.7	2600.9	0.7679	7.2234	7.9912
60	19.941	0.001017	7.671	251.09	2205.5	2456.6	251.11	2358.5	2609.6	0.8311	7.0794	7.9095
65	25.033	0.001020	6.197	272.00	2191.1	2463.1	272.03	2346.2	2618.2	0.8934	6.9375	7.8309
70	31.188	0.001023	5.042	292.93	2176.6	2469.5	292.96	2333.8	2626.8	0.9548	6.8004	7.7552
75	38.579	0.001026	4.121	312.87	2162.0	2475.0	312.91	2321.4	2635.2	1.0154	6.6670	7.6824
80	47.390	0.001029	3.407	334.84	2147.4	2482.2	334.88	2308.8	2643.7	1.0752	6.5369	7.6121
85	57.834	0.001032	2.828	355.82	2132.6	2488.4	355.88	2296.0	2651.9	1.1342	6.4102	7.5444
90	70.139	0.001036	2.361	376.82	2117.7	2494.5	376.90	2283.2	2660.1	1.1924	6.2866	7.4790
95	84.554	0.001040	1.982	397.86	2102.7	2500.6	397.94	2270.2	2668.1	1.2500	6.1659	7.4158
100	0.10135	0.001044	1.6729	418.91	2087.6	2506.5	419.02	2257.0	2676.0	1.3068	6.0480	7.3548
105	0.12082	0.001047	1.4194	440.00	2072.3	2512.3	440.13	2243.7	2683.8	1.3629	5.9328	7.2958
110	0.14328	0.001052	1.2102	461.12	2057.0	2518.1	461.27	2230.2	2691.5	1.4184	5.8202	7.2386
115	0.16906	0.001056	1.0366	482.28	2041.4	2523.7	482.46	2216.5	2699.0	1.4733	5.7100	7.1832
120	0.19853	0.001060	0.8919	503.48	2025.8	2529.2	503.69	2202.6	2706.3	1.5275	5.6020	7.1295
125	0.2321	0.001065	0.77059	524.72	2009.9	2534.6	524.96	2188.5	2713.5	1.5812	5.4962	7.0774
130	0.2701	0.001070	0.66850	546.00	1993.9	2539.9	546.29	2174.2	2720.5	1.6343	5.3925	7.0269
135	0.3130	0.001075	0.58217	567.34	1977.7	2545.0	567.67	2159.6	2727.3	1.6869	5.2907	6.9777
140	0.3613	0.001080	0.50885	588.72	1961.3	2550.0	589.11	2144.8	2733.9	1.7390	5.1908	6.9298
145	0.4154	0.001085	0.44632	610.16	1944.7	2554.9	610.61	2129.6	2740.3	1.7906	5.0926	6.8832
150	0.4759	0.001090	0.39278	631.66	1927.9	2559.5	632.18	2114.3	2746.4	1.8417	4.9960	6.8378
155	0.5431	0.001096	0.34676	653.23	1910.8	2564.0	653.82	2098.6	2752.4	1.8924	4.9010	6.7934
160	0.6178	0.001102	0.30706	674.85	1893.5	2568.4	675.53	2082.6	2758.1	1.9426	4.8075	6.7501
165	0.7005	0.001108	0.27260	696.55	1876.0	2572.5	697.32	2066.2	2763.5	1.9924	4.7153	6.7078
170	0.7917	0.001114	0.24283	718.31	1858.1	2576.5	719.20	2049.5	2768.7	2.0418	4.6244	6.6663